Robust gain-scheduling H_∞ control of uncertain continuous-time systems having magnitude- and rate-bounded actuators: an application of full block S-procedure

Kucukdemiral, Ibrahim B.; Yazici, Hakan

Published in:
Journal of the Franklin Institute

DOI:
10.1016/j.jfranklin.2021.08.017

Publication date:
2021

Document Version
Author accepted manuscript

Robust gain-scheduling $\mathcal{H}_\infty$ control of uncertain continuous-time systems having magnitude- and rate-bounded actuators: An application of full block S-procedure

Ibrahim Kucukdemiral* Hakan Yazici†

Abstract

This paper addresses a novel robust gain-scheduling(GS) state-feedback (SF) $\mathcal{H}_\infty$ (induced $\mathcal{L}_2$) control method for uncertain continuous-time(CT) systems having actuators with hard rate and magnitude bounds. The proposed method relies on acceleration form representation of the uncertain CT system. The technique enables the user to represent the control signal and its slew rate as auxiliary outputs along with the main controlled output. Two different norms, namely the induced $\mathcal{L}_\infty$ and $\mathcal{L}_2$ are used to control the system effectively. While the $\mathcal{L}_\infty$ gain from the exogenous disturbance inputs to the control signal related outputs is used to deal with actuator saturation problem, $\mathcal{L}_2$ gain from the disturbance inputs to the performance outputs is utilised in attenuation of the effects of the disturbances. To achieve these goals with minimal conservatism, we develop new forms of dilated Matrix Inequality (MI) conditions for peak-to-peak gain and $\mathcal{L}_2$ gain with no additional conservatism. Then, we propose a novel robust GS control methodology to deal with the problem via dilated MIs and a modified full block S-procedure method (MFBSPM). The utilisation of MFBSPM ensures that the robust control design method of this note applies to any uncertain system having rational parameter dependence. Finally, the efficiency of the presented method is portrayed through extensive simulations of the responses of a marine vessel to wave excitations in which the vessel model is assumed to have magnitude and rate limited active fin stabiliser.

1 Introduction

Almost all physical systems include actuators with strict magnitude and rate limitations. Also, they are affected by detrimental disturbances and model uncertainties. Most mechanical or electromechanical actuators can only provide limited force, torque, stroke under strict rate restrictions. However, these limitations are often ignored in controller design. The magnitude, and especially the rate bounds of the actuator, are identified as a serious source of undesirable transient response and may even cause closed-loop instability and poor performance in several industrial applications [24, 44]. For instance, rate saturations on the control surfaces caused YF-22 to crash in 1992 [13, 1, 8, 45]. Other practical examples of control systems in which actuator saturations appear as a major reason for instability can be given as engine compressors [49], stabilization of ships by using active fins [27] and reactors having slow actuators [10].

*Glasgow Caledonian University, School of Computing, Engineering and Built Environment, Department of Applied Science, G4 0BA, Glasgow, UK, E-mail: iku1@gcu.ac.uk

†Yildiz Technical University, School of Mechanical Engineering, Istanbul, Turkey

Therefore, designing efficient controllers for systems with limited actuators is considered a fundamental challenge for control engineers [42]. The literature has extensive results, especially for systems having actuators with only magnitude bounds [2, 52, 22, 47, 28, 11]. This problem is mainly tackled with different forms of anti-windup(AW) structures [20]. Interested readers can refer to the works of [17], [21] or [24], for a detailed overview of AW control methods.

Compared to the large number of results that exist on the design of controllers for the processes having only magnitude limited actuators, the research on systems comprising actuators with both rate and magnitude limits is insufficient, although magnitude limits generally play a less important role in closed-loop stability and performance than that of the limits on the rate of the control signal [44].

In the literature, the problem is usually handled depending on whether the system under consideration is nonlinear or linear. In the nonlinear setting, several methods are presented to provide an efficient solution to the actuator saturation problem in the literature. For instance, [30] proposes a model predictive controller (MPC) to obtain nonlinear control law that guarantees compliance to the strict magnitude and input rate constraints. A novel optimization approach is introduced by [40] for the stabilization of a class of nonlinear systems having inputs subject to magnitude and rate bounds. [48], applies a saturated sliding mode control method in which magnitude and rate limitations are formulated for systems having known and unknown bounded uncertainties. A nonlinear attractive ellipsoidal approach is proposed by [4] to avoid the hard quasi-Lipschitz assumptions. Moreover, [46] introduces a new projection algorithm for adaptive control of these systems.

Apart from the nonlinear control methods discussed above, various linear techniques have also been presented to tackle actuator the saturation problem. A group of researchers dealt with the problem via revamping AW techniques, which have been developed for magnitude bounded systems. In AW based methods, actuator limitations are not considered right away in the controller design process but mostly utilised to reduce the harmful after-effects developed by these constraints. This problem is sorted out by introducing compensation elements in the closed-loop. First, a linear compensator that does not explicitly consider the saturation constraints is produced; then, an AW extension is introduced to take care of the control input limits. Therefore, in this method, it is necessary to use additional compensation elements in the control architecture to mitigate the undesirable effects of actuator limitations. For instance, [5] proposed an AW strategy to control exponentially unstable processes having actuators with magnitude and rate limits. However, parameter robustness was not considered in their work. A new multi-stage AW technique was developed by [36] to obtain more efficient control performance and reduce the added conservatism for CT systems under consideration of peak bounded disturbance. Again, they did not touch on the robustness problem of the controller in their study. Other techniques that deal with the problem include use of saturation blocks in nested configuration [6, 43, 51, 33], nested and attractive ellipsoids [26], MPCs [31] and representation of the actuator with low order sluggish model [25, 23, 9]. Particularly, [26] considers a GS stabilisation problem in the discrete-time domain by utilising nested and invariant ellipsoids without considering any performance objectives. On the other hand, the GS technique introduced in this reference is based on a switching mechanism in which the controller changes its feedback gain depending on the existence of saturation. In their method, the GS controller's gains are pre-computed depending on the different levels of disturbances and then evaluated by a supervisory mechanism during run-time. If a saturation occurs, the supervisory mechanism switches to a lower pre-determined gain ensuring that a highest gain that is not saturated would be the one to be used at all times. Therefore, the technique used in [26] works in a way similar to the working principle of an anti wind-up (AW) mechanism and, therefore, prone to ringing problems.

Based on the literature review, we understand that the papers considering the control systems incorporating magnitude and rate saturation problem simultaneously are very rare, compared to the ones that consider only magnitude bounds. Besides, most of them attack the problem by using AW based strategies or MPC, which seldom conceive the robustness problem and the compelling effects of disturbances. Therefore, in this paper, we develop a novel and also easily realisable robust GS $\mathcal{H}_\infty$ controller for plants having strict control channel limits and subject to magnitude bounded disturbances. A new acceleration form representation of the uncertain system having three different controlled outputs is proposed and considered to handle the magnitude bounds of the control signal and its rate independently. We utilise peak-to-peak gains of the system to cope with the actuator saturation problem whereas the minimisation of the induced $\mathcal{L}_2$ gain is used to mitigate the effects of disturbances on the controlled outputs. Since most physical systems evolve naturally in continuous time, the proposed multi-objective controller is developed in CT domain. Highlights of this paper are summarised as follows:

- As opposed to the literature, we introduce a novel control design technique that does not rely on a form of AW architecture or attractive/nested ellipsoid methods. We propose a new technique that relies on multi-objective optimisation and acceleration form representation of the system having three different controlled outputs. While the actuator saturation is dealt with considering the peak-to-peak (induced $\mathcal{L}_\infty$) gain from the disturbance inputs to the controlled outputs: the control signal and its rate; a third controlled output is used to suppress the impacts of the disturbance by carrying out a minimisation of the $\mathcal{L}_2$ norm. Proposed acceleration form and defining the control constraints in terms of peak-to-peak gains from disturbances to the channels of control related outputs allow us to convert this challenging control problem to a linear multi-objective control problem which can be solved effectively by MIs.

- The proposed technique of this study relies on the peak-to-peak (induced $\mathcal{L}_\infty$) and the induced $\mathcal{L}_2$ gain conditions. To obtain a less conservative multi-objective optimisation based design method, we use dilated matrix inequalities. To this end, this paper introduces novel dilated MI conditions to calculate the upper bound of the peak-to-peak and induced $\mathcal{L}_2$ gains of a CT system without any additional conservatism.

- The controller generated by the proposed design method, always keeps the loop in the linear region by not exceeding the magnitude and rate saturations at any time. Therefore, a smooth operation is always achieved. Compared to its AW counterparts and [26], the proposed technique of this present paper does not contain any ringing problem which may lead to a discontinuity in the control signal. Hence, the proposed technique is well suited for use in mechanical systems which are prone to damage because of stringent working conditions and exposition to excessive usage.

- Extension of the proposed method to the robust design is also provided. We employ recently developed MFBSPM and dilated MIs to get a robust synthesis method that provides the least conservative controller . We stress that the linear fractional representation (LFR) of the uncertain process and the utilisation of the Pólya relaxation help us to achieve a synthesis method that can be used on any kind of uncertain process in which the parameters appear in rational parameter dependence form. Generally, these types of problems cannot be handled by other techniques in the literature without bringing up extra conservatism.

- Lastly, based on the proposed technique, a novel robust GS control method is also developed to get better performance from the controller through the LFR representation of the uncertain system.

The organisation of this paper can be summarised as follows: Control problem is stated in the next section. Then, in Section 3, we propose dilated MI based non-conservative approaches to the computation of peak-to-peak gain and induced $\mathcal{L}_2$ gain for CT, linear time-invariant systems. Section 4 expands the idea to the control of systems having control limitations. Numerical simulation results along with detailed discussions are presented in Section 5. In this section, the efficiency of the proposed approach is validated through an extensive comparison study comprising the response of uncontrolled process and that of MPC by using the roll-motion control problem of a marine vessel having model uncertainties, active fin stabiliser with restricted actuator dynamics and subject to wave-based disturbances. Finally, the paper is concluded with Section 6.

Notation $\mathbb{R}$ represents the set of real numbers whereas $\mathbb{R}^+$ symbolises the positive portion of this set. $\mathbb{Z}$ is used to represent the set of integers and $\mathbb{C}$ denotes the set of complex numbers. $\mathbb{R}^n$ represents size $n-$ real vectors. The notation $\mathbb{R}^{n\times m}$ is used to show real matrices with size $n \times m$. I represents identity matrix and $\mathbf{0}$ stands for the null matrices. For a block vector z, the notation $z_j^i \in \mathbb{R}$ stands for the $i-$th entry of the $j-$th vector entry of the vector z. G^{T} is the transpose of G. The notation $\star$ denotes symmetric blocks in an asymmetric matrix. $\mathsf{He}\{P\} = P + P^{\mathrm{T}}$. For a real valued vector $w \in \mathbb{R}^s$, $\|w\|_\infty$ represents its infinity norm which is calculated as $\|w\|_\infty = \max_{1\leq j\leq s} \sup_{t\geq 0} |w_j(t)|$. $w \in \mathcal{L}_\infty$ if $\|w\|_\infty < \infty$. The notation, $\mathsf{diag}\{\cdot\}$ represents the diagonal matrices. $\mathsf{conv}\{S\}$ represents the convex hull of S. $A \succeq (\preceq)\mathbf{0}$ denotes that A is a symmetric positive (negative) semi-definite matrix. $\mathcal{G}_{z,w}$ denotes the transfer function from w to z and $\|\mathcal{G}\|$ stands for its induced system norm. For a real valued signal x, x belongs to the set of $\mathcal{L}_2$ signals if $\|x\|_2 \triangleq \sqrt{\int_0^\infty x^{\mathrm{T}}(t)x(t)\mathrm{d}t} < \infty$. Then, we define the induced $\mathcal{L}_2$ norm of a system $\mathcal{G}$ having inputs $w \in \mathcal{L}_2$ and outputs $z \in \mathcal{L}_2$ as $\|\mathcal{G}\|_\infty = \|\mathcal{G}\|_{\mathcal{L}_2\to\mathcal{L}_2} \triangleq \sup\limits_{0\neq w\in\mathcal{L}_2} \frac{\|z\|_2}{\|w\|_2}$ and peak-to-peak (induced $\mathcal{L}_\infty$) norm as $\|\mathcal{G}\|_{\mathcal{L}_\infty\to\mathcal{L}_\infty} \triangleq \sup\limits_{0\neq w\in\mathcal{L}_\infty} \frac{\|z\|_\infty}{\|w\|_\infty}$. Finally, for a matrix $\mathcal{C}_u$, $\mathcal{C}_{u,i}$ represents its $i-$th row.

2 Problem formulation

Consider the system governed by the set of differential equations

$$\mathcal{G}\left\{\begin{array}{rcl} \dot{x}(t) &=& A(\Delta(t),\Theta(t))x(t) + B(\Delta(t),\Theta(t))u(t) + H(\Delta(t),\Theta(t))w(t) \\ z_x(t) &=& C(\Delta(t),\Theta(t))x(t) + D(\Delta(t),\Theta(t))w(t) \end{array}\right. \tag{1}$$

where $x(t) \in \mathbb{R}^n$ stands for the state vector, $u(t) \in \mathbb{R}^m$ represents the control inputs, $z_x(t) \in \mathbb{R}^p$ captures the outputs that are controlled and $w(t) \in \mathbb{R}^s$ is the disturbance input vector which satisfies $\|w\|_2 < \infty$ for all $t \geq 0$. We assume that $\|w\|_\infty \in \mathbb{R}^+$ is known. Uncertainties are captured by $\Delta(t) \in \mathbf{\Delta}$ where $\mathbf{\Delta}$ shows its compact cover, whose borders are assumed to be known. Similarly, $\Theta(t) \in \mathbf{\Theta}$ is a time-varying measurable/observable system parameter and $\mathbf{\Theta}$ is used to represent its known covering border set. $u(t)$ stands for the manipulating input whose channels $j = 1, \dots, m$ to satisfy the physical limits:

$$|u_j(t)| \le \bar{u}_j, \qquad |v_j(t)| \triangleq |\dot{u}_j(t)| \le \bar{v}_j, \tag{2}$$

for all $t \ge 0$ where $\bar{u}_j$ and $\bar{v}_j$ are known limits.

This paper aims to develop a robustly stabilising full-state feedback gain-scheduled control law for (1) that satisfies the control limits (2) for all time and minimises the impact of $w(t)$ on $z_x(t)$ in terms of the $\mathcal{L}_2$ gain. To achieve these goals with minimal conservatism, a novel robust control method based on mixed $\mathcal{L}_2/\mathcal{L}_\infty$ control with dilated MIs and S-procedure method is introduced in this note.

For the sake of simplicity, from this point onward, we shall omit to use the symbol t in our notation whenever it is obvious.

3 Preliminary results

Our method to the solution of the control problem addressed above relies on multi-objective optimisation which utilises peak-to-peak gain condition (a.k.a induced $\mathcal{L}_\infty$ norm) and induced $\mathcal{L}_2$ norm (a.k.a $\mathcal{H}_\infty$ gain) of the process. Therefore, in an attempt to obtain a controller with minimal conservatism, we introduce dilated MI characterisations of these performance measures. In a standard Linear Matrix Inequality (LMI) based controller, controller gains are always a function of the Lyapunov matrix. This turns into a problematic situation when there are multiple objectives to accomplish as the Lyapunov matrix needs to be taken common in every condition. The benefit of using a dilated versions of the MIs of performance measures is that, in contrast to the conventional MIs, the resultant controller will not be a function of the Lyapunov matrix. This allows the user to choose different Lyapunov matrices for different performance measures. Dilated versions of the controller design conditions in MI formulation can be obtained by transforming the associated Lyapunov stability conditions to generalised inequalities through the introduction of some slack variables. Discrete-time dilated LMI conditions are generally easier to develop than the CT versions, also more common and elegant [32]. In CT setting, developing non-conservative LMIs that would replace standard LMIs is not that straightforward and challenging [15]. Dilation is performed by adding slack terms to the existing LMIs in such a way that they would provide some freedom to the optimisation and therefore can provide less conservatism in the analysis and design [3], [41].

The approach introduced in this paper is based on the peak-to-peak gain of the system that requires the usage of dilated matrix inequalities(MIs) in order to minimise the conservatism. During the development of the method, we shall use the following lemma.

Lemma 1 *(Projection Lemma:) [16] Let $\mathcal{Z} = \mathcal{Z}^{\mathrm{T}}, \mathcal{U}$ and $\mathcal{V}$ be matrices in appropriate dimensions. And assume that the range spaces of $\mathcal{U}$ and $\mathcal{V}$ are independent. Then one can find a matrix $\mathcal{X}$ that satisfies*

$$\mathcal{U}^{\mathrm{T}}\mathcal{X}\mathcal{V} + \mathcal{V}^{\mathrm{T}}\mathcal{X}^{\mathrm{T}}\mathcal{U} + \mathcal{Z} \prec \mathbf{0}, \tag{3}$$

if and only if

$$\mathcal{N}_{\mathcal{U}}^{\mathrm{T}}\mathcal{Z}\mathcal{N}_{\mathcal{U}} \prec \mathbf{0}, \tag{4}$$

and

$$\mathcal{N}_{\mathcal{V}}^{\mathrm{T}}\mathcal{Z}\mathcal{N}_{\mathcal{V}} \prec \mathbf{0}, \tag{5}$$

are both satisfied. Here, $\mathcal{N}_{\mathcal{U}}$ and $\mathcal{N}_{\mathcal{V}}$ are user defined matrices whose columns span the null-spaces of the matrices $\mathcal{U}$ and $\mathcal{V}$, respectively.

The controller design approach requires the satisfaction of control constraints (2) for all $t \geq 0$. To ensure this condition at any time t, we shall employ induced $\mathcal{L}_\infty$ norm from disturbance input to the auxiliary outputs.

Theorem 1 *(Peak-to-peak bound) Given the scalar $\lambda > 0$, if one can find matrices X, $Q = Q^{\mathrm{T}}$ and $\gamma \in \mathbb{R}^+$, $\mu \in \mathbb{R}^+$ that satisfy*

$$\mathsf{He}\left\{ \begin{bmatrix} X^{\mathrm{T}}A^{\mathrm{T}} \\ -X^{\mathrm{T}} \\ H^{\mathrm{T}} \end{bmatrix} \begin{bmatrix} \lambda I & I & \mathbf{0} \end{bmatrix} \right\} - \begin{bmatrix} \lambda Q & Q & \mathbf{0} \\ Q & \mathbf{0} & \mathbf{0} \\ \mathbf{0} & \mathbf{0} & -\mu I \end{bmatrix} \succ \mathbf{0}, \tag{6}$$

$$\begin{bmatrix} \lambda Q & \mathbf{0} & X^{\mathrm{T}}C^{\mathrm{T}} \\ \mathbf{0} & (\gamma - \mu)I & D^{\mathrm{T}} \\ CX & D & \gamma I \end{bmatrix} \succ \mathbf{0}, \tag{7}$$

then, the system

$$\Sigma \left\{ \begin{array}{rcl} \dot{x} & = & Ax + Hw \\ z & = & Cx + Dw \end{array} \right. \tag{8}$$

is asymptotically stable(AS) and has a peak-to-peak gain smaller than γ.

Proof 1 *As indicated in Section 2.4.5 of the dissertation authored by [12], for a given $\lambda \in \mathbb{R}^+$, system (8) has an induced $\mathcal{L}_\infty$ (peak-to-peak) norm less than γ, if $\exists\, P = P^{\mathrm{T}} \succ \mathbf{0}$, $\gamma \in \mathbb{R}^+$ and $\mu \in \mathbb{R}^+$ that satisfy*

$$\begin{bmatrix} A^{\mathrm{T}}P + PA + \lambda P & PH \\ \star & -\mu I \end{bmatrix} \prec \mathbf{0}, \tag{9}$$

$$\begin{bmatrix} \lambda P & \mathbf{0} & C^{\mathrm{T}} \\ \mathbf{0} & (\gamma - \mu)I & D^{\mathrm{T}} \\ C & D & \gamma I \end{bmatrix} \succ \mathbf{0}. \tag{10}$$

Note that, in standard form, (9) can be expressed as

$$\mathcal{N}_{\mathcal{U}}^{\mathrm{T}} \underbrace{\begin{bmatrix} \lambda P & P & \mathbf{0} \\ P & \mathbf{0} & \mathbf{0} \\ \mathbf{0} & \mathbf{0} & -\mu I \end{bmatrix}}_{\mathcal{Z}} \underbrace{\begin{bmatrix} I & \mathbf{0} \\ A & H \\ \mathbf{0} & I \end{bmatrix}}_{\mathcal{N}_{\mathcal{U}}} \prec \mathbf{0}. \tag{11}$$

Hence, based on the structure of $\mathcal{N}_{\mathcal{U}}$, a possible selection is $\mathcal{U} = \begin{bmatrix} -A & I & -H \end{bmatrix}$.

For the stability requirements, we need to impose an additional inequality constraint which guarantees the positive definiteness of P. To this end, we shall consider a candidate basis $\mathcal{N}_{\mathcal{V}} = \begin{bmatrix} I & -\lambda I & \mathbf{0} \end{bmatrix}^{\mathrm{T}}$ which leads to

$$\mathcal{N}_{\mathcal{V}}^{\mathrm{T}} \mathcal{Z} \mathcal{N}_{\mathcal{V}} = \begin{bmatrix} I & -\lambda I & \mathbf{0} \end{bmatrix} \mathcal{Z} \begin{bmatrix} I \\ -\lambda I \\ \mathbf{0} \end{bmatrix} = -\lambda P \prec \mathbf{0}, \tag{12}$$

which guarantees the positive definiteness of P whenever $\lambda > 0$. On the other hand, a trivial inequality can also be obtained by choosing $\mathcal{N}_{\mathcal{V}} = \begin{bmatrix} \mathbf{0} & \mathbf{0} & I \end{bmatrix}^{\mathrm{T}}$ which leads to $\mathcal{N}_{\mathcal{V}}^{\mathrm{T}} \mathcal{Z} \mathcal{N}_{\mathcal{V}} = -\mu I \prec \mathbf{0}$. Hence, in line with these selections for the basis of $\mathcal{N}_{\mathcal{V}}$, one viable combined choice for the basis of the null space of $\mathcal{V}$ could be $\mathcal{N}_{\mathcal{V}} = \begin{bmatrix} I & -\lambda I & \mathbf{0} \\ \mathbf{0} & \mathbf{0} & I \end{bmatrix}^{\mathrm{T}}$, which leads to an orthogonal matrix $\mathcal{V} = \begin{bmatrix} \lambda I & I & \mathbf{0} \end{bmatrix}$. In line with the selections of the matrices $\mathcal{U}$ and $\mathcal{V}$, and Lemma 3, (9) is identical to the presence of an unstructured matrix $\mathcal{X}$ satisfying

$$\mathsf{He}\left\{ \begin{bmatrix} -A^{\mathrm{T}} \\ I \\ -H^{\mathrm{T}} \end{bmatrix} \mathcal{X} \begin{bmatrix} \lambda I & I & \mathbf{0} \end{bmatrix} \right\} + \begin{bmatrix} \lambda P & P & \mathbf{0} \\ P & \mathbf{0} & \mathbf{0} \\ \mathbf{0} & \mathbf{0} & -\mu I \end{bmatrix} \prec \mathbf{0}. \tag{13}$$

Then, respectively, defining $X \triangleq \mathcal{X}^{-1}$, $Q \triangleq X^{\mathrm{T}} P X$ and applying a congruence transformation on (13) with $\mathsf{diag}\{X, X, I\}$ and its transpose gives (6). Here, one can infer from (13) that the congruence transformation is always viable since $\mathcal{X}^{\mathrm{T}} + \mathcal{X} \prec 0$ and therefore $\mathcal{X}$ is full rank.

Similarly, applying a congruence transformation on inequality (10) by using $\mathsf{diag}\{X, I, I\}$ and its transpose yields (7). This completes our proof.

If one replaces A with $A + BK$ in (8) and (6) and utilises the definition $L \triangleq KX$ in its place, a SF controller can be obtained for the nominal open-loop system

$$\begin{aligned} \dot{x} &= Ax + Bu + Hw \\ z &= Cx + Dw \end{aligned} \tag{14}$$

which guarantees that the peak-to-peak norm from w to z is less than γ.

Corollary 2 *Given the scalar $\lambda > 0$, if $\exists\, X$, L, $Q = Q^{\mathrm{T}}$ and $\gamma \in \mathbb{R}^+$ and $\mu \in \mathbb{R}^+$ which satisfy*

$$\mathsf{He}\left\{ \begin{bmatrix} X^{\mathrm{T}} A^{\mathrm{T}} + L^{\mathrm{T}} B^{\mathrm{T}} \\ -X^{\mathrm{T}} \\ H^{\mathrm{T}} \end{bmatrix} \begin{bmatrix} \lambda I & I & \mathbf{0} \end{bmatrix} \right\} - \begin{bmatrix} \lambda Q & Q & \mathbf{0} \\ Q & \mathbf{0} & \mathbf{0} \\ \mathbf{0} & \mathbf{0} & -\mu I \end{bmatrix} \succ \mathbf{0}, \tag{15}$$

and

$$\begin{bmatrix} \lambda Q & \mathbf{0} & X^{\mathrm{T}} C^{\mathrm{T}} \\ \mathbf{0} & (\gamma - \mu) I & D^{\mathrm{T}} \\ CX & D & \gamma I \end{bmatrix} \succ \mathbf{0}, \tag{16}$$

then, the closed-loop system

$$\begin{aligned} \dot{x} &= (A + BK)x + Hw \\ z &= Cx + Dw \end{aligned} \tag{17}$$

is AS; has a peak-to-peak gain smaller than γ and $K = LX^{-1}$.

In an attempt to obtain a controller which attenuates the effects of disturbance w on the controlled output z_x, we shall employ $\mathcal{H}_\infty$ characterization of the system norm. Therefore, next, we will develop lossless dilated LMI conditions to compute this norm and then extend the result to the design of a SF controller through a corollary.

Theorem 3 *(Bounded real-lemma with dilated matrix inequalities) For a given scalar $\gamma_\infty \in \mathbb{R}^+$, Σ governed by differential equations (8) has $\|\Sigma\|_\infty < \gamma_\infty$ if and only if $\exists\, \lambda \in \mathbb{R}^+$ and matrices X, $G = G^{\mathrm{T}} \succ 0$ that satisfy*

$$\mathsf{He}\left\{ \begin{bmatrix} X^{\mathrm{T}}A^{\mathrm{T}} \\ -X^{\mathrm{T}} \\ H^{\mathrm{T}} \\ \mathbf{0} \end{bmatrix} \begin{bmatrix} \lambda I & I & \mathbf{0} & \mathbf{0} \end{bmatrix} \right\} - \begin{bmatrix} \mathbf{0} & G & \mathbf{0} & \star \\ G & \mathbf{0} & \mathbf{0} & \mathbf{0} \\ \mathbf{0} & \mathbf{0} & -\gamma_\infty^2 I & D^{\mathrm{T}} \\ CX & \mathbf{0} & D & -I \end{bmatrix} \succ \mathbf{0}. \tag{18}$$

Proof 2 *Let $V = x^{\mathrm{T}}Wx$ is the Lyapunov function and $W = W^{\mathrm{T}} \succ \mathbf{0}$. Then, $\|\Sigma\|_\infty < \gamma_\infty$ if and only if for all $t \geq 0$,*

$$\dot{V} + z^{\mathrm{T}}z - \gamma_\infty^2 w^{\mathrm{T}}w < 0, \tag{19}$$

is satisfied along the system trajectory (8) (see Section 6.3.2 of [7]). Note that one can easily rewrite the inequality condition (19) along the system trajectory (8) as follows:

$$\mathcal{N}_{\mathcal{U}}^{\mathrm{T}} \underbrace{\begin{bmatrix} I & \mathbf{0} & \mathbf{0} \\ \mathbf{0} & I & \mathbf{0} \\ \mathbf{0} & \mathbf{0} & I \\ C & \mathbf{0} & D \end{bmatrix}^{\mathrm{T}} \begin{bmatrix} \mathbf{0} & W & \mathbf{0} & \mathbf{0} \\ W & \mathbf{0} & \mathbf{0} & \mathbf{0} \\ \mathbf{0} & \mathbf{0} & -\gamma_\infty^2 I & \mathbf{0} \\ \mathbf{0} & \mathbf{0} & \mathbf{0} & I \end{bmatrix} \begin{bmatrix} I & \mathbf{0} & \mathbf{0} \\ \mathbf{0} & I & \mathbf{0} \\ \mathbf{0} & \mathbf{0} & I \\ C & 0 & D \end{bmatrix}}_{\mathcal{Z}} \underbrace{\begin{bmatrix} I & \mathbf{0} \\ A & H \\ \mathbf{0} & I \end{bmatrix}}_{\mathcal{N}_{\mathcal{U}}} \prec \mathbf{0}, \tag{20}$$

where

$$\mathcal{Z} = \begin{bmatrix} C^{\mathrm{T}}C & W & C^{\mathrm{T}}D \\ W & \mathbf{0} & \mathbf{0} \\ D^{\mathrm{T}}C & \mathbf{0} & D^{\mathrm{T}}D - \gamma_\infty^2 I \end{bmatrix}. \tag{21}$$

We will follow Extension-IV introduced by [35] in order to obtain equivalent conditions which won't introduce any conservatism. Comparing (20) with (11), since the left and right multipliers are identical in both inequalities, one can simply choose $\mathcal{U} = \begin{bmatrix} -A & I & -H \end{bmatrix}$. Similarly, choosing $\mathcal{N}_{\mathcal{V}} = \begin{bmatrix} I & -\lambda I & \mathbf{0} \\ \mathbf{0} & \mathbf{0} & I \end{bmatrix}^{\mathrm{T}}$, leads to the strict matrix inequality $\mathbf{0} \prec C^{\mathrm{T}}C \prec 2\lambda W$, the trivial inequality $\mathbf{0} \prec \gamma_\infty^2 I - D^{\mathrm{T}}D$ and

$$C^{\mathrm{T}}C - C^{\mathrm{T}}DED^{\mathrm{T}}C \prec 2\lambda W, \tag{22}$$

in which we used the definition $E \triangleq (D^{\mathrm{T}}D - \gamma_\infty^2 I)^{-1}$. Note that $E \prec 0$ is already implied by the original LMI (20). Defining $\epsilon \triangleq 0.5\lambda^{-1}$, the first condition can be rewritten as $\mathbf{0} \prec \epsilon C^{\mathrm{T}}C \prec W$. Hence, choosing ϵ sufficiently small, leads to the strict inequality $\mathbf{0} \prec W$ which is also imposed by the selection of V. On the other hand, $D^{\mathrm{T}}D \prec \gamma_\infty^2$ is immediately implied by the standard condition 20.

Finally, dividing both sides of (22) by 2λ and using the definition of ϵ, (22) is equivalent to

$$\epsilon(C^{\mathrm{T}}C - C^{\mathrm{T}}DED^{\mathrm{T}}C) \prec W. \tag{23}$$

The left-hand side of (23) can be less than or equal to zero or strictly greater than zero depending on the matrices C and D. The first case immediately leads to $W \succ \mathbf{0}$. In the latter case, left-hand side of (23) can be made arbitrarily small by adjusting ϵ so that the condition boils down to the strict inequality $W \succ \mathbf{0}$. Therefore, the conditions imposed by dilation do not introduce any conservatism.

Hence, once again, one can choose $\mathcal{V} = \begin{bmatrix}\lambda I & I & \mathbf{0}\end{bmatrix}$*, and based on the Lemma 3, one can infer that*

$$\mathsf{He}\left\{\begin{bmatrix}-A^{\mathrm{T}}\\ I\\ -H^{\mathrm{T}}\end{bmatrix}\mathcal{X}\begin{bmatrix}\lambda I & I & \mathbf{0}\end{bmatrix}\right\} + \begin{bmatrix}C^{\mathrm{T}}C & W & C^{\mathrm{T}}D\\ W & \mathbf{0} & \mathbf{0}\\ D^{\mathrm{T}}C & \mathbf{0} & D^{\mathrm{T}}D-\gamma_\infty^2 I\end{bmatrix} \prec \mathbf{0}, \tag{24}$$

Then, respectively, defining $X \triangleq \mathcal{X}^{-1}$*,* $G \triangleq X^{\mathrm{T}}WX$ *and applying a congruence transformation on (24) with a transformation matrix* $\mathsf{diag}\{X, X, I\}$ *gives*

$$\mathsf{He}\left\{\begin{bmatrix}-X^{\mathrm{T}}A^{\mathrm{T}}\\ X^{\mathrm{T}}\\ -H^{\mathrm{T}}\end{bmatrix}\begin{bmatrix}\lambda I & I & \mathbf{0}\end{bmatrix}\right\} + \begin{bmatrix}X^{\mathrm{T}}C^{\mathrm{T}}CX & G & \star\\ G & \mathbf{0} & \mathbf{0}\\ D^{\mathrm{T}}CX & \mathbf{0} & D^{\mathrm{T}}D-\gamma_\infty^2 I\end{bmatrix} \prec \mathbf{0}. \tag{25}$$

Finally, application of Schur complement formulae on (25) gives (18). This concludes the proof.

Then, for the nominal system (14), exchanging A in (18) with $A + BK$ and introducing extra variable $L \triangleq KX$ in its place, one can obtain an $\mathcal{L}_2$ controller in the structure of $u = Kx$ by using the following Corollary:

Corollary 4 *(17) is AS and has an* $\mathcal{L}_2$ *gain from* w *to* z *less than* $\gamma_\infty \in \mathbb{R}^+$*, if and only if* $\exists\, \lambda \in \mathbb{R}^+$ *and matrices* X*,* $G = G^{\mathrm{T}} \succ \mathbf{0}$ *and* L *such that*

$$\mathsf{He}\left\{\begin{bmatrix}X^{\mathrm{T}}A^{\mathrm{T}} + L^{\mathrm{T}}B^{\mathrm{T}}\\ -X^{\mathrm{T}}\\ H^{\mathrm{T}}\\ \mathbf{0}\end{bmatrix}\begin{bmatrix}\lambda I & I & \mathbf{0} & \mathbf{0}\end{bmatrix}\right\} - \begin{bmatrix}\mathbf{0} & G & \mathbf{0} & \star\\ G & \mathbf{0} & \mathbf{0} & \mathbf{0}\\ \mathbf{0} & \mathbf{0} & -\gamma_\infty^2 I & D^{\mathrm{T}}\\ CX & \mathbf{0} & D & -I\end{bmatrix} \succ \mathbf{0}. \tag{26}$$

Then, the controller is given by $u = Kx = LX^{-1}x$*.*

Having developed the dilated MI conditions and associated SF control law for the given peak-to-peak and $\mathcal{L}_2$ gains, next, we shall introduce a controller design method for the problem stated in Section 2.

4 Control of magnitude- and rate-bounded systems

Next, we will consider the augmented plant with an extended state vector $\bar{x}$ comprising x, u and $v \triangleq \dot{u}$, with a view to constrain the magnitude and the rate of the control signal utilizing induced $\mathcal{L}_\infty$ norm of the system while minimizing the induced $\mathcal{L}_2$ norm from w to z_x.

$$\begin{aligned}
\underbrace{\begin{bmatrix}\dot{x}\\ \dot{u}\\ \dot{v}\end{bmatrix}}_{\dot{\bar{x}}} &= \underbrace{\begin{bmatrix}A(\Delta,\Theta) & B(\Delta,\Theta) & \mathbf{0}\\ \mathbf{0} & \mathbf{0} & I\\ \mathbf{0} & \mathbf{0} & \mathbf{0}\end{bmatrix}}_{\mathcal{A}(\Delta,\Theta)}\underbrace{\begin{bmatrix}x\\ u\\ v\end{bmatrix}}_{\bar{x}} + \underbrace{\begin{bmatrix}\mathbf{0}\\ \mathbf{0}\\ I\end{bmatrix}}_{\mathcal{B}}\psi + \underbrace{\begin{bmatrix}H(\Delta,\Theta)\\ \mathbf{0}\\ \mathbf{0}\end{bmatrix}}_{\mathcal{H}(\Delta,\Theta)} w\\
\begin{bmatrix}z_x\\ z_u\\ z_v\end{bmatrix} &= \begin{bmatrix}\mathcal{C}_x(\Delta,\Theta)\\ \mathcal{C}_u\\ \mathcal{C}_v\end{bmatrix}\bar{x} + \begin{bmatrix}D(\Delta,\Theta)\\ \mathbf{0}\\ \mathbf{0}\end{bmatrix} w.
\end{aligned} \tag{27}$$

In this representation, ψ can be considered as the manipulated control input of the augmented plant (27) or an interim control signal for (1). The overall feedback interconnection is shown in

Figure 1. In this diagram, blue blocks correspond to the controller and the yellow ones stand for the process to be controlled. Signal routes in red are used only in GS controller mechanism where Θ represents the vector of measurable scheduling parameters. Note that, this augmentation allows

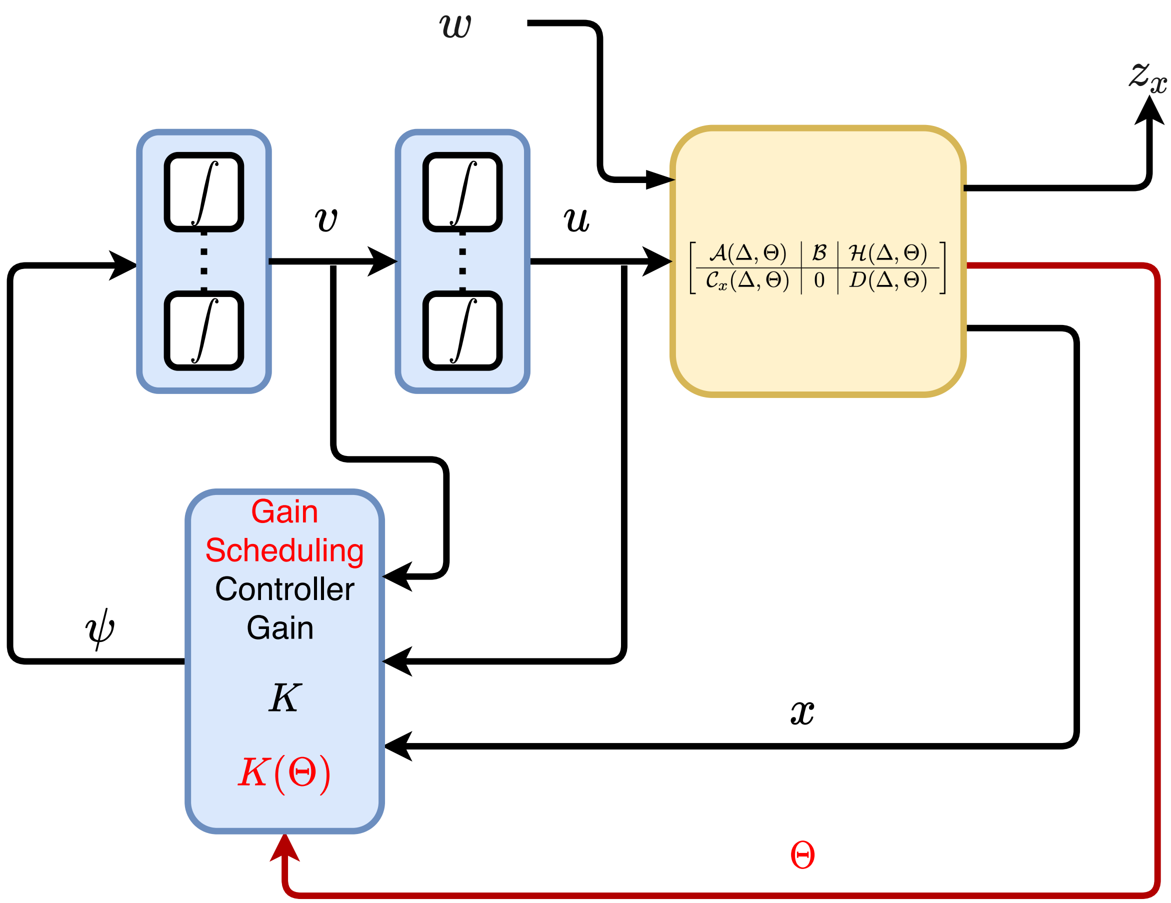

Figure 1: Control system topology.

us define u and v as new extended state variables. Thus, one can introduce auxiliary outputs $z_u \triangleq u$ and $z_v \triangleq v$ along with the original controlled output z_x using the matrix definitions $\mathcal{C}_x(\Delta,\Theta) = \begin{bmatrix} C(\Delta,\Theta) & \mathbf{0}_{p\times m} & \mathbf{0}_{p\times m} \end{bmatrix}$, $\mathcal{C}_u = \begin{bmatrix} \mathbf{0}_{m\times n} & I_m & \mathbf{0}_{m\times m} \end{bmatrix}$ and $\mathcal{C}_v = \begin{bmatrix} \mathbf{0}_{m\times n} & \mathbf{0}_{m\times m} & I_m \end{bmatrix}$. Then, whenever the magnitude bound $(\bar{u}_i)$ and the rate bound $(\bar{v}_i)$ of the $i-$th channel of the control vector are given as in (2), and the peak norm of the disturbance signal, $\|w\|_\infty$ is known, one can set the allowable maximum peak-to-peak gain from w to the $i-$th channel of z_u to

$$\gamma = \frac{\bar{u}_i}{\|w\|_\infty}, \quad i = 1, \ldots, m. \tag{28}$$

Similarly, one can set the peak-to-peak gain from w to the $i-$th channel of the controlled output z_v to

$$\gamma = \frac{\bar{v}_i}{\|w\|_\infty}, \quad i = 1, \ldots, m. \tag{29}$$

Then, any control signal ψ, and therefore the actual control signal u, designed in such a way that it attenuates the impacts of w on the controlled output z_x and satisfies the peak-to-peak gain constraints (28) and (29), will never exceed the amplitude and rate limits on the control signal. Note that, once a controller is designed for (27), one can easily recover the original control signal as $u = \iint \psi$.

The aim is to obtain a control law of the form $u = \mathcal{K}(\bar{x})$ that mitigates the induced $\mathcal{L}_2$ gain γ_∞ from the channel w to z_x while satisfying the control signal constraints defined in (2) at all times. One way to achieve this is seeking the minimum achievable gain γ_∞ while ensuring that the closed-loop peak-to-peak gains satisfy $\|\mathcal{G}_{z_u^i,w}\|_{\mathcal{L}_\infty\to\mathcal{L}_\infty} = \bar{u}_i/\|w\|_\infty$ and $\|\mathcal{G}_{z_v^i,w}\|_{\mathcal{L}_\infty\to\mathcal{L}_\infty} = \bar{v}_i/\|w\|_\infty$ for each control channel $i = 1,\dots,m$.

Choosing $A = A(\Delta,\Theta)$, $H = H(\Delta,\Theta)$ constant at their nominal values, the following theorem provides an $\mathcal{L}_2$ controller for the nominal version of the system governed by (1).

Theorem 5 *For given scalars $\lambda \in \mathbb{R}^+$ and $\gamma_\infty \in \mathbb{R}^+$, there exists a SF controller for (1) that ensures $\|\mathcal{G}\|_\infty < \gamma_\infty$ and conform to the control constraints (2), if $\exists\, \mu \in \mathbb{R}^+$, matrices L, X, $Q = Q^{\mathrm{T}} \succ \mathbf{0}$ and $G = G^{\mathrm{T}} \succ \mathbf{0}$ satisfying*

$$\mathsf{He}\left\{\begin{bmatrix} X^{\mathrm{T}}\mathcal{A}^{\mathrm{T}} + L^{\mathrm{T}}\mathcal{B}^{\mathrm{T}} \\ -X^{\mathrm{T}} \\ \mathcal{H}^{\mathrm{T}} \end{bmatrix}\begin{bmatrix}\lambda I & I & \mathbf{0}\end{bmatrix}\right\} - \begin{bmatrix} \lambda Q & Q & \mathbf{0} \\ Q & \mathbf{0} & \mathbf{0} \\ \mathbf{0} & \mathbf{0} & -\mu I \end{bmatrix} \succ \mathbf{0}, \tag{30}$$

$$\begin{bmatrix} \lambda Q & \mathbf{0} & X^{\mathrm{T}}\mathcal{C}_{u,i}^{\mathrm{T}} \\ \mathbf{0} & \left(\frac{\bar{u}_i}{\|w\|_\infty} - \mu\right) I & \mathbf{0} \\ \mathcal{C}_{u,i}X & \mathbf{0} & \frac{\bar{u}_i}{\|w\|_\infty} I \end{bmatrix} \succ \mathbf{0}, \quad \forall\, i = 1,\dots,m \tag{31}$$

$$\begin{bmatrix} \lambda Q & \mathbf{0} & X^{\mathrm{T}}\mathcal{C}_{v,i}^{\mathrm{T}} \\ \mathbf{0} & \left(\frac{\bar{v}_i}{\|w\|_\infty} - \mu\right) I & \mathbf{0} \\ \mathcal{C}_{v,i}X & \mathbf{0} & \frac{\bar{v}_i}{\|w\|_\infty} I \end{bmatrix} \succ \mathbf{0}, \quad \forall\, i = 1,\dots,m \tag{32}$$

and

$$\mathsf{He}\left\{\begin{bmatrix} X^{\mathrm{T}}\mathcal{A}^{\mathrm{T}} + L^{\mathrm{T}}\mathcal{B}^{\mathrm{T}} \\ -X^{\mathrm{T}} \\ \mathcal{H}^{\mathrm{T}} \\ \mathbf{0} \end{bmatrix}\begin{bmatrix}\lambda I & I & \mathbf{0} & \mathbf{0}\end{bmatrix}\right\} - \begin{bmatrix} \mathbf{0} & G & \mathbf{0} & X^{\mathrm{T}}\mathcal{C}_x^{\mathrm{T}} \\ G & \mathbf{0} & \mathbf{0} & \mathbf{0} \\ \mathbf{0} & \mathbf{0} & -\gamma_\infty^2 I & D^{\mathrm{T}} \\ \mathcal{C}_x X & \mathbf{0} & D & -I \end{bmatrix} \succ \mathbf{0}. \tag{33}$$

Then, the controller can be obtained as $u = \iint K\bar{x} = \iint LX^{-1}\bar{x}$. Here, $\bar{x}$ is the augmented state vector described in (27).

Proof 3 *We shall consider the system defined by (27). Since we have two separate conditions on the control signal, namely the magnitude and rate bounds, one needs to apply Corollary 2 two times for each $i = 1,\dots,m$; by first taking $\gamma \triangleq \bar{u}_i/\|w\|_\infty$, and then $\gamma \triangleq \bar{v}_i/\|w\|_\infty$. It follows from the conditions of Corollary 2 that (30), (31) and (32) guarantee that magnitude and rate bounds are not violated at any time $t \geq 0$. Finally, following the LMI condition in Corollary 4, a feasible solution to the inequality (33) guarantees that the closed-loop interconnection from w to the output z_x, has an $\mathcal{L}_2$ gain less than γ_∞.*

4.1 Robust Control

In the case of existence of uncertainties in the model description, we represent the plant matrices which depend on parameter matrix compactly by Linear Fractional Transformation (LFT) [14] [37] as follows:

$$\left[\begin{array}{c|c}\mathcal{A}(\Delta) & \mathcal{H}(\Delta)\\ \hline \mathcal{C}_x(\Delta) & D(\Delta)\end{array}\right] = \left[\begin{array}{c|c}\mathcal{A} & \mathcal{H}\\ \hline \mathcal{C}_x & D\end{array}\right] + \left[\begin{array}{c}\mathcal{N}\\ \hline \mathcal{M}\end{array}\right] \Delta \left[I - \mathcal{W}\Delta\right]^{-1} \left[\Upsilon \quad | \quad \Omega\right], \tag{34}$$

where $\mathcal{N}$, $\mathcal{M}$, $\mathcal{W}$, $\mathcal{U}$ and $\mathcal{V}$ are all known matrices of appropriate dimensions which can be obtained from the LFR of the uncertain system matrices. Note that the model can be rationally dependent on uncertainty matrix Δ satisfying $\Delta \in \mathbf{\Delta}$, $\forall\, t \geq 0$. Here, $\mathbf{\Delta}$ is assumed to be a compact cover set whose borders are known. Note that since our method relies on the employment of full block S-procedure technique, our proposition does not require a particular formation in $\mathbf{\Delta}$.

As a means to obtain a robust GS control configuration in the form of $u = \mathcal{K}(\bar{x})$ with minimum conservatism, we adapt MFBSPM [38] technique to the derivation. Note that relaxation of parameter-dependent LMIs with full block scaling matrices instead of using D-G scales provide more freedom in the design and therefore less conservatism [18].

In an attempt to develop the main result, we shall hire the following Lemma 2. However, first, we introduce a matrix Φ satisfying

$$\begin{bmatrix}\bar{\Delta}^{\mathrm{T}}\\ I\end{bmatrix}^{\mathrm{T}} \underbrace{\begin{bmatrix}\Psi & \chi\\ \chi^{\mathrm{T}} & \Pi\end{bmatrix}}_{\Phi} \begin{bmatrix}\bar{\Delta}^{\mathrm{T}}\\ I\end{bmatrix} \preceq 0,\ \forall\, \bar{\Delta} \in \mathbf{\Delta}. \tag{35}$$

Besides, we need to introduce the following definition of LFT using star product:

$$\bar{\Delta} \star \underbrace{\left[\begin{array}{c|c}\mathcal{Y}_{11} & \mathcal{Y}_{12}\\ \hline \mathcal{Y}_{21} & \mathcal{Y}_{22}\end{array}\right]}_{\mathcal{Y}} \triangleq \mathcal{Y}_{22} + \mathcal{Y}_{21}\bar{\Delta}(I - \mathcal{Y}_{11}\bar{\Delta})^{-1}\mathcal{Y}_{12}, \tag{36}$$

which is defined as a well-posed interconnection whenever the matrix $(I - \mathcal{Y}_{11}\bar{\Delta})$ is nonsingular for every $\bar{\Delta} \in \bar{\mathbf{\Delta}}$.

Lemma 2 *(Lemma 7 of [18]) The following are equivalent:*

(i) $\bar{\Delta} \star \mathcal{Y}$ *is well-posed and*

$$\mathsf{He}\{\bar{\Delta} \star \mathcal{Y}\} \succeq \mathbf{0},\ \bar{\Delta} \in \bar{\mathbf{\Delta}}, \tag{37}$$

(ii) A block-structured matrix Φ *exists that satisfies (35) and*

$$\begin{bmatrix}\mathcal{Y}_{21}\Pi\mathcal{Y}_{21}^{\mathrm{T}} + \mathsf{He}\{\mathcal{Y}_{22}\} & \mathcal{Y}_{21}\Pi\mathcal{Y}_{11}^{\mathrm{T}} + \mathcal{Y}_{21}\chi^{\mathrm{T}} + \mathcal{Y}_{12}^{T}\\ * & \Psi + \mathcal{Y}_{11}\Pi\mathcal{Y}_{11}^{\mathrm{T}} + \mathsf{He}\{\mathcal{Y}_{11}\chi^{\mathrm{T}}\}\end{bmatrix} \succeq \mathbf{0}. \tag{38}$$

Having provided the ingredients above, now one can establish the following theorem:

Theorem 6 *For a given $\lambda \in \mathbb{R}^+$, A robust SF controller for uncertain process (1) exists that ensures $\|\mathcal{G}\|_\infty < \gamma_\infty$ and complies with the control constraints (2), if $\exists\, \mu \in \mathbb{R}^+$, matrices L, X, $Q = Q^{\mathrm{T}} \succ \mathbf{0}$, $G = G^{\mathrm{T}} \succ \mathbf{0}$, $\Pi_j = \Pi_j^{\mathrm{T}}$, $\Psi_j = \Psi_j^{\mathrm{T}}$, χ_j, that satisfy (31), (32), (35) along with*

$$\begin{bmatrix} \mathcal{Y}_{21}^j \Pi_j \left(\mathcal{Y}_{21}^j\right)^{\mathrm{T}} + \mathsf{He}\{\mathcal{Y}_{22}^j\} & \mathcal{Y}_{21}^j \Pi_j \mathcal{Y}_{11}^{\mathrm{T}} + \mathcal{Y}_{21}^j \chi_j^{\mathrm{T}} + \left(\mathcal{Y}_{12}^j\right)^{\mathrm{T}} \\ * & \Psi_j + \mathcal{Y}_{11} \Pi_j \mathcal{Y}_{11}^{\mathrm{T}} + \mathsf{He}\{\mathcal{Y}_{11} \chi_j^{\mathrm{T}}\} \end{bmatrix} \succeq \mathbf{0}, \tag{39}$$

for all $j = 1, 2$ where

$$\mathsf{He}\{\mathcal{Y}_{22}^1\} = \mathsf{He}\left\{ \begin{bmatrix} \lambda I \\ I \\ \mathbf{0} \end{bmatrix} \begin{bmatrix} \mathcal{A}X + \mathcal{B}L & -X & \mathcal{H} \end{bmatrix} \right\} - \begin{bmatrix} \lambda Q & Q & \mathbf{0} \\ Q & \mathbf{0} & \mathbf{0} \\ \mathbf{0} & \mathbf{0} & -\mu I \end{bmatrix}, \tag{40}$$

$$\mathcal{Y}_{21}^1 = \begin{bmatrix} \lambda \mathcal{N} \\ \mathcal{N} \\ \mathbf{0} \end{bmatrix}, \quad \mathcal{Y}_{11} = \mathcal{W}, \quad \mathcal{Y}_{12}^1 = \begin{bmatrix} \Upsilon X & \mathbf{0} & \Omega \end{bmatrix}, \tag{41}$$

$$\mathsf{He}\{\mathcal{Y}_{22}^2\} = \mathsf{He}\left\{ \begin{bmatrix} \lambda I \\ I \\ \mathbf{0} \\ \mathbf{0} \end{bmatrix} \begin{bmatrix} \mathcal{A}X + \mathcal{B}L & -X & \mathcal{H} & \mathbf{0} \end{bmatrix} \right\} - \begin{bmatrix} \mathbf{0} & G & \mathbf{0} & X^{\mathrm{T}} \mathcal{C}_x^{\mathrm{T}} \\ G & \mathbf{0} & \mathbf{0} & \mathbf{0} \\ \mathbf{0} & \mathbf{0} & -\gamma_\infty^2 I & D^{\mathrm{T}} \\ \mathcal{C}_x X & \mathbf{0} & D & -I \end{bmatrix}, \tag{42}$$

$$\mathcal{Y}_{21}^2 = \begin{bmatrix} \lambda \mathcal{N} \\ \mathcal{N} \\ \mathbf{0} \\ \mathcal{M} \end{bmatrix}, \quad \mathcal{Y}_{12}^2 = \begin{bmatrix} \Upsilon X & \mathbf{0} & \Omega & \mathbf{0} \end{bmatrix}. \tag{43}$$

Then, the controller can be obtained as $u = \iint K\bar{x} = \iint LX^{-1}\bar{x}$. Here, $\bar{x}$ is the augmented state vector described in (27).

Proof 4 *In accordance with the decomposition of the uncertain matrices in (34), (30) can be expressed as*

$$\underbrace{\mathsf{He}\left\{ \begin{bmatrix} \lambda I \\ I \\ \mathbf{0} \end{bmatrix} \begin{bmatrix} \mathcal{A}X + \mathcal{B}L & -X & \mathcal{H} \end{bmatrix} \right\} - \begin{bmatrix} \lambda Q & Q & \mathbf{0} \\ Q & \mathbf{0} & \mathbf{0} \\ \mathbf{0} & \mathbf{0} & -\mu I \end{bmatrix}}_{\mathsf{He}\{\mathcal{Y}_{22}^1\}}$$

$$+ \mathsf{He}\left\{ \underbrace{\begin{bmatrix} \lambda \mathcal{N} \\ \mathcal{N} \\ \mathbf{0} \end{bmatrix}}_{\mathcal{Y}_{21}^1} \underbrace{\Delta}_{\bar{\Delta}} \Big(I - \underbrace{\mathcal{W}}_{\mathcal{Y}_{11}} \Delta \Big)^{-1} \underbrace{\begin{bmatrix} \Upsilon X & \mathbf{0} & \Omega \end{bmatrix}}_{\mathcal{Y}_{12}^1} \right\} \succ 0. \tag{44}$$

Similarly, the matrix inequality (33) can be represented as

$$\underbrace{\mathsf{He}\left\{\begin{bmatrix}\lambda I\\ I\\ \mathbf{0}\\ \mathbf{0}\end{bmatrix}\begin{bmatrix}\mathcal{A}X+\mathcal{B}L & -X & \mathcal{H} & \mathbf{0}\end{bmatrix}\right\}-\begin{bmatrix}\mathbf{0} & G^{\mathrm{T}} & \mathbf{0} & \star\\ G & \mathbf{0} & \mathbf{0} & \mathbf{0}\\ \mathbf{0} & \mathbf{0} & -\gamma_\infty^2 I & D^{\mathrm{T}}\\ \mathcal{C}_x X & \mathbf{0} & D & -I\end{bmatrix}}_{\mathsf{He}\{\mathcal{Y}_{22}^2\}}$$
$$+\mathsf{He}\left\{\underbrace{\begin{bmatrix}\lambda\mathcal{N}\\ \mathcal{N}\\ \mathbf{0}\\ \mathcal{M}\end{bmatrix}}_{\mathcal{Y}_{21}^2}\underbrace{\Delta}_{\bar{\Delta}}\left(I-\underbrace{\mathcal{W}}_{\mathcal{Y}_{11}}\Delta\right)^{-1}\underbrace{\begin{bmatrix}\Upsilon X & \mathbf{0} & \Omega & \mathbf{0}\end{bmatrix}}_{\mathcal{Y}_{12}^2}\right\}\succ\mathbf{0}. \quad (45)$$

Finally, application of Lemma 2 on (44) and (45) and using the matrix definitions of $\mathcal{Y}$ above yield (39). This concludes the proof.

4.2 Robust and GS control

Let the system matrices in (1) are decomposed as follows:

$$\left[\begin{array}{c|c}\mathcal{A}(\Delta,\Theta) & \mathcal{H}(\Delta,\Theta)\\ \hline \mathcal{C}_x(\Delta,\Theta) & D(\Delta,\Theta)\end{array}\right]=\left[\begin{array}{c|c}\mathcal{A} & \mathcal{H}\\ \hline \mathcal{C}_x & D\end{array}\right]$$
$$+\left[\begin{array}{c|c}\mathcal{N} & \mathcal{J}\\ \hline \mathcal{M} & \mathcal{F}\end{array}\right]\begin{bmatrix}\Delta & \mathbf{0}\\ \mathbf{0} & \Theta\end{bmatrix}\left(\begin{bmatrix}I & \mathbf{0}\\ \mathbf{0} & I\end{bmatrix}-\begin{bmatrix}\mathcal{W} & \mathbf{0}\\ \mathbf{0} & \mathcal{R}\end{bmatrix}\begin{bmatrix}\Delta & \mathbf{0}\\ \mathbf{0} & \Theta\end{bmatrix}\right)^{-1}\left[\begin{array}{c|c}\Upsilon & \Omega\\ \hline \mathcal{E} & \mathcal{T}\end{array}\right], \quad (46)$$

where $\Delta \in \mathbf{\Delta}$ represents the system uncertainties and $\Theta \in \mathbf{\Theta}$ are the measurable scheduling parameter matrix.

Theorem 7 *Given $\gamma_\infty \in \mathbb{R}^+$ and $\lambda \in \mathbb{R}^+$, $\exists$ a robust GS SF controller for uncertain system (1) that ensures $\|\mathcal{G}\|_\infty < \gamma_\infty$ and complies with the control constraints (2), if $\exists\,\mu \in \mathbb{R}^+$, matrices L_1, L_2, X, $Q = Q^{\mathrm{T}} \succ \mathbf{0}$, $G = G^{\mathrm{T}} \succ \mathbf{0}$, $\Pi_j = \Pi_j^{\mathrm{T}}$, $\Psi_j = \Psi_j^{\mathrm{T}}$, χ_j, which satisfy (31), (32), (35) along with*

$$\begin{bmatrix}\mathcal{Y}_{21}^j\Pi_j\left(\mathcal{Y}_{21}^j\right)^{\mathrm{T}}+\mathsf{He}\{\mathcal{Y}_{22}^j\} & \mathcal{Y}_{21}^j\Pi_j\mathcal{Y}_{11}^{\mathrm{T}}+\mathcal{Y}_{21}^j\chi_j^{\mathrm{T}}+\left(\mathcal{Y}_{12}^j\right)^{\mathrm{T}}\\ * & \Psi_j+\mathcal{Y}_{11}\Pi_j\mathcal{Y}_{11}^{\mathrm{T}}+\mathsf{He}\{\mathcal{Y}_{11}\chi_j^{\mathrm{T}}\}\end{bmatrix}\succeq\mathbf{0}, \quad (47)$$

for all $j = 1, 2$ and

$$\mathcal{Y}_{11}=\begin{bmatrix}\mathcal{W} & \mathbf{0} & \mathbf{0}\\ \mathbf{0} & \mathcal{R} & \mathbf{0}\\ \mathbf{0} & \mathbf{0} & \mathcal{R}^{\mathrm{T}}\end{bmatrix}, \quad \bar{\Delta}=\begin{bmatrix}\Delta & \mathbf{0} & \mathbf{0}\\ \mathbf{0} & \Theta & \mathbf{0}\\ \mathbf{0} & \mathbf{0} & \Theta^{\mathrm{T}}\end{bmatrix}, \quad (48)$$

$$\mathsf{He}\{\mathcal{Y}_{22}^1\}=\mathsf{He}\left\{\begin{bmatrix}\lambda I\\ I\\ \mathbf{0}\end{bmatrix}\begin{bmatrix}\mathcal{A}X+L_1^{\mathrm{T}}\mathcal{B}^{\mathrm{T}} & -X & \mathcal{H}\end{bmatrix}\right\}-\begin{bmatrix}\lambda Q & Q & \mathbf{0}\\ Q & \mathbf{0} & \mathbf{0}\\ \mathbf{0} & \mathbf{0} & -\mu I\end{bmatrix}, \quad (49)$$

$$\mathcal{Y}_{21}^1 = \begin{bmatrix} \lambda\mathcal{N} & \lambda\mathcal{J} & \lambda\mathcal{J} \\ \mathcal{N} & \mathcal{J} & \mathcal{J} \\ \mathbf{0} & \mathbf{0} & \mathbf{0} \end{bmatrix}, \quad \mathcal{Y}_{12}^1 = \begin{bmatrix} \Upsilon X & \mathbf{0} & \Omega \\ \mathcal{E}X & \mathbf{0} & \mathcal{T} \\ L_2^{\mathrm{T}}\mathcal{B}^{\mathrm{T}} & \mathbf{0} & \mathbf{0} \end{bmatrix}, \tag{50}$$

$$\mathsf{He}\{\mathcal{Y}_{22}^2\} = \mathsf{He}\left\{ \begin{bmatrix} \lambda I \\ I \\ \mathbf{0} \\ \mathbf{0} \end{bmatrix} \begin{bmatrix} \mathcal{A}X + L_1^{\mathrm{T}}\mathcal{B}^{\mathrm{T}} & -X & \mathcal{H} & \mathbf{0} \end{bmatrix} \right\} - \begin{bmatrix} \mathbf{0} & G^{\mathrm{T}} & \mathbf{0} & X^{\mathrm{T}}\mathcal{C}_x^{\mathrm{T}} \\ G & \mathbf{0} & \mathbf{0} & \mathbf{0} \\ \mathbf{0} & \mathbf{0} & -\gamma_\infty^2 I & D^{\mathrm{T}} \\ \mathcal{C}_x X & \mathbf{0} & D & -I \end{bmatrix}, \tag{51}$$

$$\mathcal{Y}_{21}^2 = \begin{bmatrix} \lambda\mathcal{N} & \lambda\mathcal{J} & \lambda\mathcal{J} \\ \mathcal{N} & \mathcal{J} & \mathcal{J} \\ \mathbf{0} & \mathbf{0} & \mathbf{0} \\ \mathcal{M} & \mathcal{F} & \mathbf{0} \end{bmatrix}, \quad \mathcal{Y}_{12}^2 = \begin{bmatrix} \Upsilon X & \mathbf{0} & \Omega & \mathbf{0} \\ \mathcal{E}X & \mathbf{0} & \mathcal{T} & \mathbf{0} \\ L_2^{\mathrm{T}}\mathcal{B}^{\mathrm{T}} & \mathbf{0} & \mathbf{0} & \mathbf{0} \end{bmatrix}. \tag{52}$$

Then, one can construct the controller as $u = \iint L(\Theta)X^{-1}\bar{x}$ *where* $L(\Theta) = L_1 + L_2(I - \Theta\mathcal{R})^{-1}\Theta\mathcal{J}^{\mathrm{T}}$. *Here,* $\bar{x}$ *is the augmented state vector described in (27).*

Proof 5 *Let us write the feedback gain matrix in the form of*

$$L^{\mathrm{T}}(\Theta) = L_1^{\mathrm{T}} + \mathcal{J}\Theta^{\mathrm{T}}\left(I - \mathcal{R}^{\mathrm{T}}\Theta^{\mathrm{T}}\right)^{-1} L_2^{\mathrm{T}}. \tag{53}$$

Then, using the uncertain matrix decompositions (46), matrix inequality (30) can be written as

$$\begin{aligned} &\underbrace{\mathsf{He}\left\{ \begin{bmatrix} \lambda I \\ I \\ \mathbf{0} \end{bmatrix} \begin{bmatrix} \mathcal{A}X + L_1^{\mathrm{T}}\mathcal{B}^{\mathrm{T}} & -X & \mathcal{H} \end{bmatrix} \right\} - \begin{bmatrix} \lambda Q & Q & \mathbf{0} \\ Q & \mathbf{0} & \mathbf{0} \\ \mathbf{0} & \mathbf{0} & -\mu I \end{bmatrix}}_{\mathsf{He}\{\mathcal{Y}_{22}^1\}} \\ &+ \mathsf{He}\left\{ \underbrace{\begin{bmatrix} \lambda\mathcal{N} & \lambda\mathcal{J} & \lambda\mathcal{J} \\ \mathcal{N} & \mathcal{J} & \mathcal{J} \\ \mathbf{0} & \mathbf{0} & \mathbf{0} \end{bmatrix}}_{\mathcal{Y}_{21}^1} \underbrace{\begin{bmatrix} \Delta & \mathbf{0} & \mathbf{0} \\ \mathbf{0} & \Theta & \mathbf{0} \\ \mathbf{0} & \mathbf{0} & \Theta^{\mathrm{T}} \end{bmatrix}}_{\bar{\Delta}} \right. \\ &\left. \times \left(I - \underbrace{\begin{bmatrix} \mathcal{W} & \mathbf{0} & \mathbf{0} \\ \mathbf{0} & \mathcal{R} & \mathbf{0} \\ \mathbf{0} & \mathbf{0} & \mathcal{R}^{\mathrm{T}} \end{bmatrix}}_{\mathcal{Y}_{11}} \begin{bmatrix} \Delta & \mathbf{0} & \mathbf{0} \\ \mathbf{0} & \Theta & \mathbf{0} \\ \mathbf{0} & \mathbf{0} & \Theta^{\mathrm{T}} \end{bmatrix} \right)^{-1} \underbrace{\begin{bmatrix} \Upsilon X & \mathbf{0} & \Omega \\ \mathcal{E}X & \mathbf{0} & \mathcal{T} \\ L_2^{\mathrm{T}}\mathcal{B}^{\mathrm{T}} & \mathbf{0} & \mathbf{0} \end{bmatrix}}_{\mathcal{Y}_{12}^1} \right\} \succ 0. \end{aligned} \tag{54}$$

Besides, the matrix inequality (33) can be represented as

$$\underbrace{\mathsf{He}\left\{\begin{bmatrix}\lambda I\\ I\\ \mathbf{0}\\ \mathbf{0}\end{bmatrix}\begin{bmatrix}\mathcal{A}X+L_1^{\mathrm{T}}\mathcal{B}^{\mathrm{T}} & -X & \mathcal{H} & \mathbf{0}\end{bmatrix}\right\}-\begin{bmatrix}\mathbf{0} & G^{\mathrm{T}} & \mathbf{0} & X^{\mathrm{T}}\mathcal{C}_x^{\mathrm{T}}\\ G & \mathbf{0} & \mathbf{0} & \mathbf{0}\\ \mathbf{0} & \mathbf{0} & -\gamma_\infty^2 I & D^{\mathrm{T}}\\ \mathcal{C}_x X & \mathbf{0} & D & -I\end{bmatrix}}_{\mathsf{He}\{\mathcal{Y}_{22}^2\}}$$

$$+\,\mathsf{He}\left\{\underbrace{\begin{bmatrix}\lambda\mathcal{N} & \lambda\mathcal{J} & \lambda\mathcal{J}\\ \mathcal{N} & \mathcal{J} & \mathcal{J}\\ \mathbf{0} & \mathbf{0} & \mathbf{0}\\ \mathcal{M} & \mathcal{F} & \mathbf{0}\end{bmatrix}}_{\mathcal{Y}_{21}^2}\bar{\Delta}\left(I-\mathcal{Y}_{11}\bar{\Delta}\right)^{-1}\underbrace{\begin{bmatrix}\Upsilon X & \mathbf{0} & \Omega & \mathbf{0}\\ \mathcal{E}X & \mathbf{0} & \mathcal{T} & \mathbf{0}\\ L_2^{\mathrm{T}}\mathcal{B}^{\mathrm{T}} & \mathbf{0} & \mathbf{0} & \mathbf{0}\end{bmatrix}}_{\mathcal{Y}_{12}^2}\right\}\succ\mathbf{0}. \quad (55)$$

Finally, application of Lemma 2 on (54) and (55) and using the matrix definitions of $\mathcal{Y}$ given above, yield (47).

Remark 1 *We note that for all admissible values of $\bar{\Delta}\in\bar{\mathbf{\Delta}}$, (35) needs to be satisfied. However, a feasibility check with an infinite number of MI conditions is impractical and computationally infeasible. Therefore, a finite number of conditions are needed to represent (35). For this purpose, several relaxation methods can be used to ensure the satisfaction of the condition (35). For polytopic regions, one can employ convex-hull relaxation or Pólya's approach. On the other hand, for sectors characterised by polynomial inequalities, it would be more suitable to use the sum-of-squares (SOS) method. For details, the reader is invited to see [34] and [39]) and the references therein. In this work, we employed Pólya relaxation for checking the feasibility of the infinite-dimensional MI condition (35). The details of the application is presented in Section 5.1.2 of the paper by [26].*

5 Illustrative Example

In the present section, the efficiency and applicability of the proposed control algorithms are exhibited through an example that considers the roll-motion control of a marine vessel having 1DOF roll dynamics and an active fin stabiliser. The simulations are performed in MATLAB environment by using the parser YALMIP [29] and the solvers SeDuMi and MOSEK. All solutions to the ordinary differential equations are obtained using a strict version of the solver ode15 which is also known as `ode15s` in MATLAB. In all simulation studies, the effectiveness of the proposed technique is compared with those of an offset-free disturbance rejection type MPC introduced in the recent paper by [27] by discretising the plant by backward Euler's method with a sampling period of 0.01s.

To that end, in a model predictive control setup, defining $k\in\mathbb{Z}$ as the sampling instant and $\Delta u(k)\triangleq u(k)-u(k-1)$, the MPC problem, which needs to be solved in every iteration k, can be summarised as follows:

$$\begin{aligned}
\underset{\Delta u(k),\ldots,\Delta u(k+N_u-1)}{\text{minimise}} \quad & \tfrac{1}{2} z_x^T(k+N)\mathcal{S} z_x(k+N) + \tfrac{1}{2}\textstyle\sum_{i=0}^{N-1} z_x^T(k+i)\mathcal{Q} z_x(k+i) \\
& + \tfrac{1}{2}\textstyle\sum_{i=0}^{N_u-1} \Delta u^T(k+i)\mathcal{R}\Delta u(k+i) \\
\text{subject to} \quad & x(k+1) = Ax(k) + Bu(k) + Hw(k) \\
& z_x = Cx(k) + Dw(k) \\
& \text{Control constraints: (2)}
\end{aligned} \tag{56}$$

for all $i = 0, \ldots, N_u - 1$. Here, $N \in \mathbb{Z}$ symbolises the prediction horizon and $N_u \leq N$ stands for the control horizon. Besides, $\mathcal{S} = \mathcal{S}^{\mathrm{T}} \succeq 0$, $\mathcal{Q} = \mathcal{Q}^{\mathrm{T}} \succeq 0$ and $\mathcal{R} = \mathcal{R}^{\mathrm{T}} \succ 0$. Once an optimal solution $\Delta^\star u(k)$ is obtained, the control signal that needs to be applied to the system (1) can be recovered as $u(k) = u(k-1) + \Delta^\star u(k)$.

For demonstration purposes, we shall use the following vessel model considered in [19] and [50]:

$$\frac{\mathrm{d}}{\mathrm{d}t}\begin{bmatrix} x_1 \\ x_2 \\ x_3 \\ x_4 \end{bmatrix} = \underbrace{\begin{bmatrix} 0 & 1 & 0 & 0 \\ a_1(t) & a_2(t) & a_3 & 0 \\ 0 & 0 & a_4(t) & 0 \\ \tau & 0 & 0 & -\tau \end{bmatrix}}_{A} \underbrace{\begin{bmatrix} x_1 \\ x_2 \\ x_3 \\ x_4 \end{bmatrix}}_{x} + \underbrace{\begin{bmatrix} 0 \\ 0 \\ b(t) \\ 0 \end{bmatrix}}_{B} u + \underbrace{\begin{bmatrix} 0 \\ 1 \\ 0 \\ 0 \end{bmatrix}}_{H} w, \tag{57}$$

$$z = \underbrace{\begin{bmatrix} 0 & 0 & 0 & 1 \end{bmatrix}}_{C} x + \underbrace{\begin{bmatrix} 0 \end{bmatrix}}_{D} w. \tag{58}$$

Here, x_1 stands for the roll angle (in rad), x_2 stands for the roll rate (in rad/s) and x_3 represents the actual actuator fin angle in radians. $1/\tau$ is the time-constant of the filter which is used in frequency shaping during the design. The aim is adjusting the fin deflection u so that x_1 follows the reference signal, which is equal to zero when the vessel is subject to stochastic wave-based disturbances of the form

$$w(t) = F_w \sin(\omega_e t), \tag{59}$$

where $F_w = 0.006$ is the wave magnitude, ω_e is the encounter frequency (in rad/s). ω_e is stochastically spread in the range $0.3 - 1.3$ rad/s. Based on the model considered by [50], the nominal values of the system parameters a_1, a_2, a_3 and b are taken as follows: $\bar{a}_1 = -0.0106$, $\bar{a}_2 = -0.1117$, $a_3 = -0.043$, $\bar{b} = 0.5$. For better regulation, we used a low pass filter having a time constant $1/\tau = 20$. In this paper, different from the literature, a realistic fin machinery model is considered. To this end, we model the fin machinery as a sluggish model having a time-constant $\bar{a}_4 = -0.5$ at its nominal value. On the other hand, it is assumed that the magnitude and the rate of fin motion are restricted with symmetric physical bounds $\bar{u} = 30^\circ$ and $\bar{v} = 20^\circ/\mathrm{s}$, respectively. Following the definition of $\mathcal{L}_2$ norm, we set all initial conditions to zero during the simulations.

In an attempt to reduce computational complexity, during the simulation studies, a common full-block uncertainty multiplier matrix $\Phi = \left[\begin{smallmatrix} \Psi & \chi \\ \chi^{\mathrm{T}} & \Pi \end{smallmatrix}\right]$ is used in all matrix inequalities having uncertain terms in (40) of Theorem 6, and (47) of Theorem 7. However, one can always assign different multiplier matrix Φ for each matrix inequality to further reduce conservatism. In this paper, we will consider three different scenarios. In the first case, we assume that the system dynamics (57) has constant system parameters at their nominal values as given above. Application of Theorem 5 yields an induced $\mathcal{L}_2$ gain $\gamma_\infty = 4.1277$ at $\lambda = 0.23$ with a control gain matrix

$$K = LX^{-1} = \begin{bmatrix} 1.83 & 7.26 & -0.47 & 3.46 & -0.47 & -0.27 \end{bmatrix} \times 10^5. \tag{60}$$

The optimal value of λ is obtained by employing a line search over a region that provides a feasible solution to the MI problem. The line search is performed by first selecting a positive interval $[\lambda_{\min}, \lambda_{\max}]$ and then dividing this interval to $N \in \mathbb{Z}$ distinct numbers. Subsequently, for each feasible value of λ and associated $\mathcal{L}_2$ gain γ_∞ is recorded and the λ that provides the minimum $\mathcal{L}_2$ gain γ_∞ is used in the controller design. For instance, in this specific case study, $\lambda \in [0.04 - 0.45]$ provided feasible solutions. The proposed controller of this note provides $\|x_1\|_2 = 0.82$ compared to $\|x_1\|_2 = 4.03$ obtained at the uncontrolled case. This corresponds to an improvement of 80% in the performance. Similarly, repeating the simulation study with an MPC provides a performance of $\|x_1\|_2 = 0.80$ compared to $\|x_1\|_2 = 3.71$ obtained at the uncontrolled case. This corresponds to control efficiency of 79%. Figure 2 demonstrates x_1 for a duration of 2000 seconds considering the controlled, uncontrolled and MPC scenarios. It is apparent that the proposed controller demonstrates a very successful rejection of the wave-based disturbances and stabilises the roll dynamics with a similar performance to that of an MPC. Besides, Figure 3 displays the control signal u and its derivative for both control topologies. While the MPC uses control energy of $\|u\| = 9.62$, the proposed controller only uses energy of $\|u\| = 0.2175$. During the simulations of MPC, control parameters are selected as $N = 20$, $N_u = 5$, $\mathcal{S} = \mathcal{Q} = CC^{\mathrm{T}}$ where $C = \left[\begin{smallmatrix} 0 & 0 & 0 & 1 \\ 0 & 1 & 0 & 0 \end{smallmatrix}\right]$, and $\mathcal{R} = 1$.

As a second case study, we consider system (57) to be uncertain with unknown parameters

$$\begin{aligned} a_i(t) &= \bar{a}_i + 0.05\bar{a}_i\delta_{ai}(t), \quad i = 1,2,4 \\ b(t) &= \bar{b} + 0.25\bar{b}\delta_b(t) \end{aligned} \tag{61}$$

where $\bar{a}_i$ shows the nominal value of the i-th parameter; δ_{ai} and δ_b are uncertain parameters which satisfy $\delta_{ai}(t) \in [-1, 1]$ for every $i = 1, 2, 4$ and $\delta_b(t) \in [-1, 1]$. Then, based on the parameter uncertainties defined in (61) and the definition $\Delta = \mathsf{diag}\{\delta_{a1}(t), \delta_{a2}(t), \delta_{a4}(t), \delta_b(t)\}$ yield uncertain system matrices of (34) as follows:

$$\mathcal{N} = \begin{bmatrix} 0 & 0 & 0 & 0 \\ 0.0230 & 0.0747 & 0 & 0 \\ 0 & 0 & 0.1581 & 0.3536 \\ 0 & 0 & 0 & 0 \\ 0 & 0 & 0 & 0 \\ 0 & 0 & 0 & 0 \end{bmatrix}, \ \mathcal{M} = \mathbf{0}_{1\times 4}, \ \mathcal{W} = \mathbf{0}_{4\times 4}, \ \Omega = \mathbf{0}_{4\times 1}, \tag{62}$$

$$\Upsilon = \begin{bmatrix} 0.0230 & 0 & 0 & 0 & 0 & 0 \\ 0 & 0.0747 & 0 & 0 & 0 & 0 \\ 0 & 0 & 0.1581 & 0 & 0 & 0 \\ 0 & 0 & 0 & 0 & 0.3536 & 0 \end{bmatrix}. \tag{63}$$

Hence, application of Theorem 6 provides minimum achievable $\mathcal{L}_2$ gain $\gamma_\infty = 8.02$ at $\lambda = 0.19$.

Furthermore, the controller gains are obtained as follows:

$$K = \begin{bmatrix} 0.3612 & 1.6694 & -0.1070 & 0.4767 & | & -0.0981 & | & -0.0491 \end{bmatrix} \times 10^6. \tag{64}$$

This controller provides an energy of $\|x_1\|_2 = 1.04$ for the controlled case compared to $\|x_1\|_2 = 4.29$ obtained for the uncontrolled case. This shows that by using the proposed robust controller algorithm, one can obtain around 76% of improvement in reduction of the energy of the roll motion.

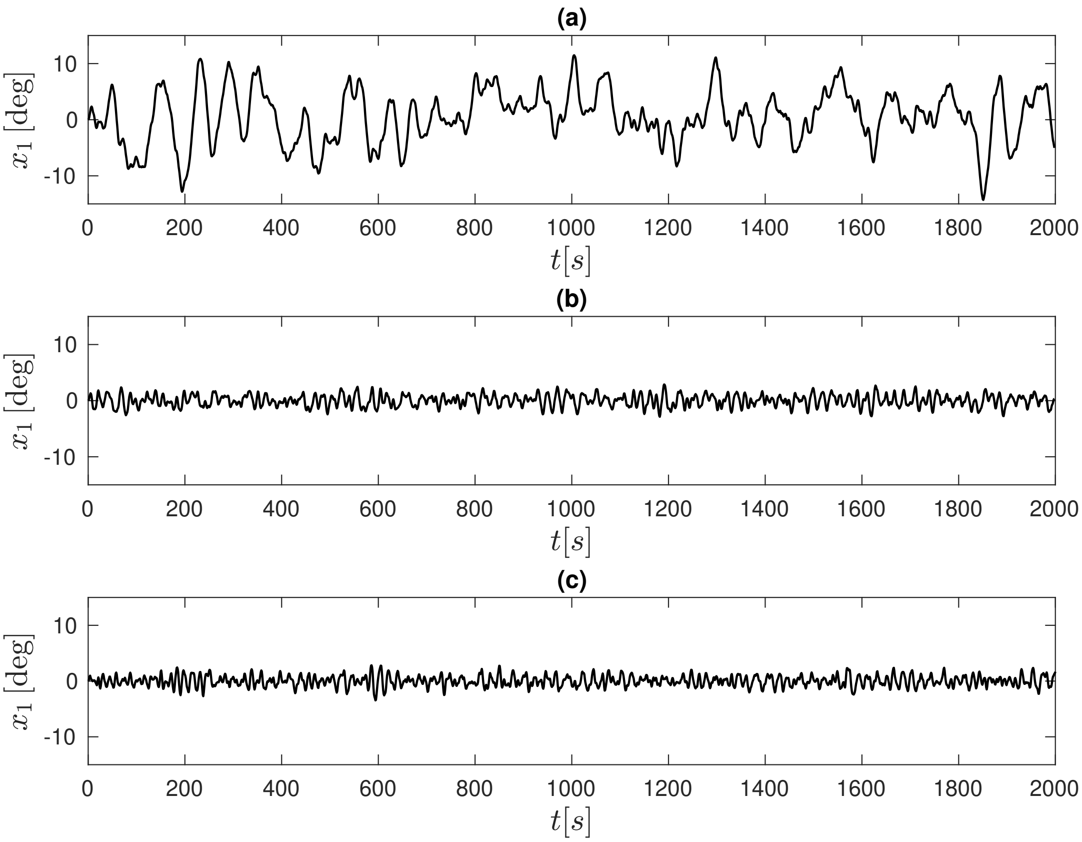

Figure 2: Nominal case: Fluctuation of the roll angle x_1: (**a**) uncontrolled case, (**b**) proposed controller (**c**) MPC.

Similarly, using the MPC with the same settings as above, we obtain $\|x_1\|_2 = 0.86$ compared to the uncontrolled scenario, which provides $\|x_1\|_2 = 3.84$. This corresponds to an improvement of 78% over the uncontrolled case. As expected, similar to the proposed controller, the efficiency of the MPC slightly reduces in the uncertain parameter case. Figure 4 shows the variation of the roll angle for a duration of 2000s for the controlled and uncontrolled cases and Figure 5 demonstrates the variations of u and its derivative. Similar to the nominal case, a satisfactory disturbance rejection performance is achieved by the proposed controller within the control signal bounds and almost identical to the performance of an advanced MPC.

During these simulation studies, in an attempt to interpret the effects of sea conditions on the system parameters at different frequencies, we used an uncertainty parameter matrix Δ selected as

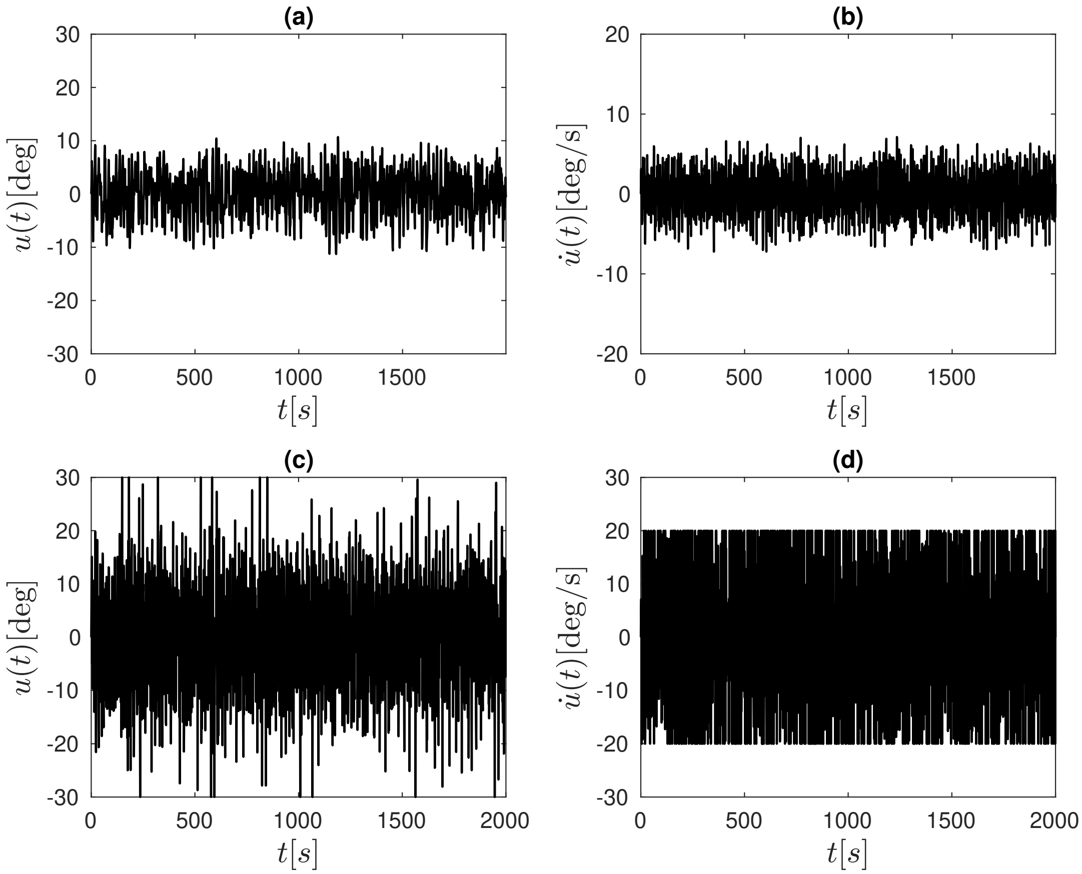

Figure 3: Nominal case: (**a**) Control signal for the proposed controller, (**b**) Derivative of the control signal for the proposed controller, (**c**) Control signal for the MPC, (**d**) Rate of the control signal associated with MPC.

follows:

$$\Delta(t) \triangleq \mathbf{diag}\{\delta_{a1}(t), \delta_{a12}(t), \delta_{a4}(t), \delta_{b}(t)\}$$
$$= \begin{bmatrix} \sin(0.03t) & 0 & 0 & 0 \\ 0 & \sin(0.6t) & 0 & 0 \\ 0 & 0 & \sin(1.3t) & 0 \\ 0 & 0 & 0 & \sin(t) \end{bmatrix}. \tag{65}$$

As a final case study, we consider the demonstration of the algorithm proposed for the design of robust and GS controller in Section 4.2. To this end, we choose the uncertain parameters as in the previous case study (61) for the a_i, $i = 1, 2, 4$ and different from the previous case the gain of the fin machinery, $b(t)$ is a measurable varying system parameter which can deviate up to 25% from its nominal value $\bar{b} = 0.5$. Therefore, similar to the uncertain system parameters a_i, where $i = 1, 2, 4$, $b(t)$ can be represented as $b(t) = \bar{b}(1 + 0.25\Theta(t))$, where $\Theta(t) \in [-1, 1]$. Then, based on these definitions of uncertain and scheduling parameters, one can obtain system matrices in (46)

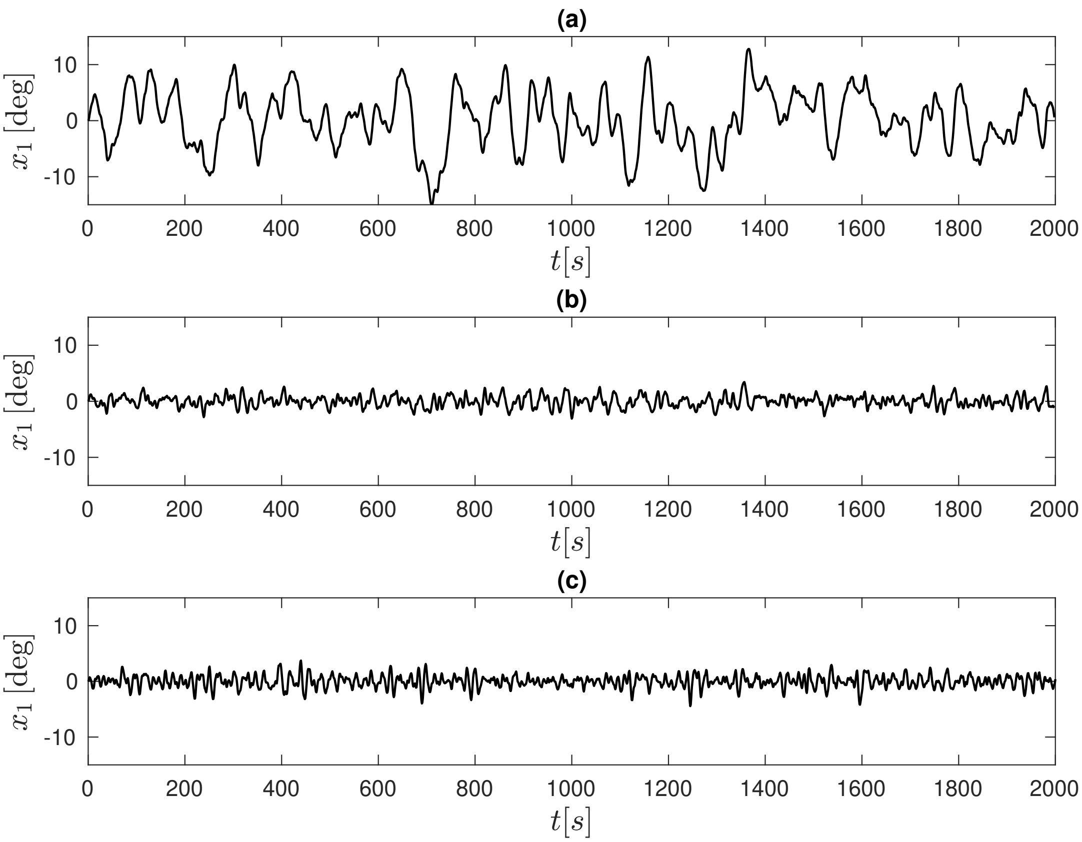

Figure 4: Uncertain parameters case: Fluctuation of x_1: for the (**a**) uncontrolled case, (**b**) proposed controller (**c**) MPC.

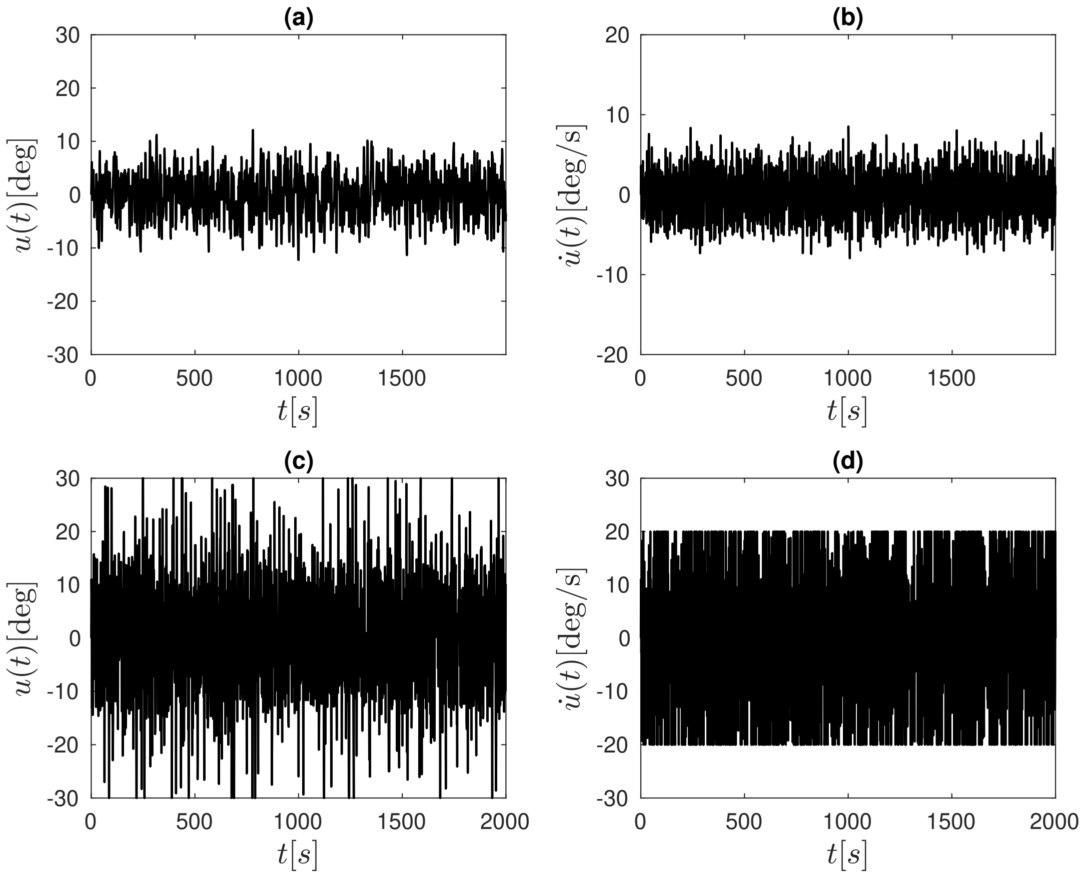

Figure 5: Uncertain parameters case: Time history of the control signals: (**a**) Control signal for the proposed controller, (**b**) Rate of control signal for the proposed controller, (**c**) Control signal for MPC, (**d**) Rate of the control signal for MPC.

as follows:

$$\mathcal{N} = \begin{bmatrix} 0 & 0 & 0 \\ 0.0230 & 0.0747 & 0 \\ 0 & 0 & 0.1581 \\ 0 & 0 & 0 \\ 0 & 0 & 0 \\ 0 & 0 & 0 \end{bmatrix}, \quad \mathcal{M} = \mathbf{0}_{1\times 3}, \quad \mathcal{W} = \mathbf{0}_{3\times 3}, \quad \Omega = \mathbf{0}_{3\times 1}, \tag{66}$$

$$\Upsilon = \begin{bmatrix} 0.0230 & 0 & 0 & 0 & 0 & 0 \\ 0 & 0.0747 & 0 & 0 & 0 & 0 \\ 0 & 0 & 0.1581 & 0 & 0 & 0 \end{bmatrix}, \ \mathcal{J} = \begin{bmatrix} 0 & 0 & 0.3536 & 0 & 0 & 0 \end{bmatrix}^{\mathrm{T}}, \tag{67}$$

$$\mathcal{R} = \mathcal{F} = \mathcal{T} = 0, \quad \mathcal{E} = \begin{bmatrix} 0 & 0 & 0 & 0 & 0.3536 & 0 \end{bmatrix}. \tag{68}$$

As in the previous case, during all simulations, we choose the variation of uncertain parameters as in (65) and the scheduling parameter as $\Theta(t) = \sin t$. Hence, application of Theorem 7 yields the minimum achievable value for the induced $\mathcal{L}_2$ as $\gamma_\infty = 11$ for $\lambda = 0.26$. On the other hand, the proposed GS controller matrices are obtained as follows:

$$\begin{aligned} L_1 &= \begin{bmatrix} -87 & 7 & -53.4 & 13.4 & -1260 & 4851408 \end{bmatrix}, \\ L_2 &= -658, \\ X &= \begin{bmatrix} -1.0477 & 0.0084 & -0.6935 & 0.3215 & -1.9162 & 1.2357 \\ 0.5926 & -0.1476 & -0.3266 & -0.0839 & 0.1477 & -0.6288 \\ 3.7532 & -2.0352 & -15.3008 & -0.2355 & -8.6058 & -1.0728 \\ -0.1020 & 0.0522 & 0.0402 & -0.0479 & 0.2087 & -0.1270 \\ 1.7476 & -0.1012 & 9.6339 & -0.1835 & -0.5701 & -13.7269 \\ -0.0911 & 0.2558 & 0.4232 & -0.0494 & 13.9330 & -954.0893 \end{bmatrix}. \end{aligned} \tag{69}$$

Figure 6 shows the variation of the roll angle for a duration of 2000 seconds together with the control signals. Simulation results confirm that the proposed robust GS control strategy is very effective in reducing the roll motion of the vessel. Application of the proposed robust GS mechanism demonstrates $\|x_1\|_2 = 0.76$ compared to $\|x_1\|_2 = 3.99$ obtained at the uncontrolled case. This result shows a dramatic improvement of 81% over the uncontrolled case.

6 Conclusion

We introduced a novel robust GS $\mathcal{H}_\infty$ controller design method for actuator saturated uncertain CT systems subject to energy and peak limited disturbances. In contrast to the literature, where AW, MPC or attractive ellipsoid based methods are mostly used, in this note, we proposed an augmented acceleration form representation of the uncertain system to tackle magnitude and rate bounds in terms of peak-to-peak gains of the system along with the induced $\mathcal{L}_2$ gain control to minimise the effects of disturbance on the controlled-outputs. In an attempt to obtain design inequalities with minimal conservatism, dilated MIs were employed during the derivation of the method. Moreover, the adaptation of MFBSPM and a Pólya relaxation enables the user to solve the problem in finite time. Thanks to the LFR representation of uncertainties, the proposed design method applies to any kind of system having rational or affine parameter dependence. The applicability and efficiency

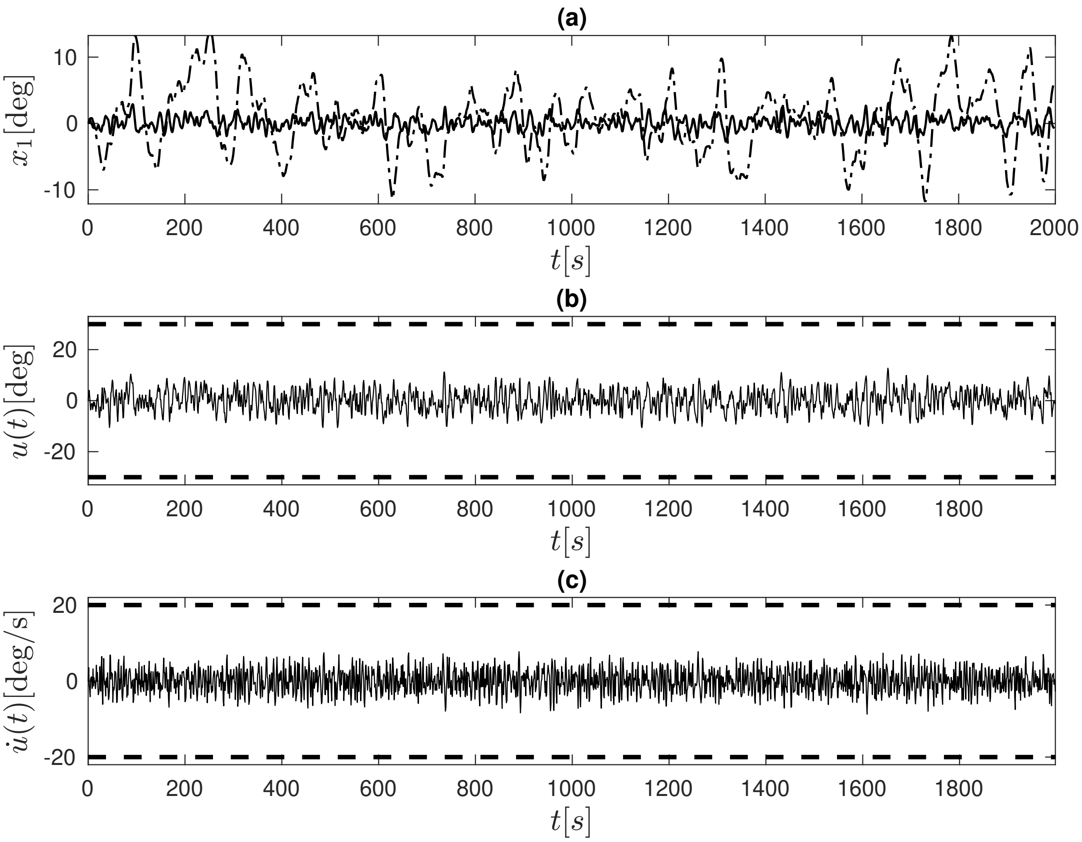

Figure 6: Robust GS control: (**a**) Variation of roll angle x_1 for the controlled case (solid black) vs to that of uncontrolled case (dashed-dot), (**b**) Variation of the control signal (**c**) Variation of the rate of the control signal. Dot-dashed lines represent actuator bounds.

of the proposed synthesis method are demonstrated by a numerical roll motion control problem of a marine vessel in comparison to that of an MPC. Extensive simulation studies exhibit that the proposed control method is very effective in reducing roll motions of marine vessels and guarantees closed-loop stability even under bounded uncertainty and the practical limitations imposed by magnitude and rate bounded actuators. A possible future extension can be developing an output feedback GS controller that employs parameter-dependent Lyapunov functions.

References

[1] Diana M. Acosta, Yildiray Yildiz, Robert W. Craun, Steven D. Beard, Michael W. Leonard, Gordon H. Hardy, and Michael Weinstein. Piloted evaluation of a control allocation technique to recover from pilot-induced oscillations. *Journal of Aircraft*, 52(1):130–140, jan 2015.

[2] J Adamy and A Flemming. Soft variable-structure controls: A survey. *Automatica*,

40(11):1821–1844, 2004.

[3] P. Apkarian, Hoang Duong Tuan, and J. Bernussou. Continuous-time analysis, eigenstructure assignment, and $\mathcal{H}_2$ synthesis with enhanced Linear Matrix Inequalities (LMI) characterizations. *IEEE Transactions on Automatic Control*, 46(12):1941–1946, 2001.

[4] V. Azhmyakov, M. Mera, and R. Juárez. Advances in attractive ellipsoid method for robust control design. *International Journal of Robust and Nonlinear Control*, 29(5):1418–1436, 2019.

[5] C. Barbu, R. Reginatto, A. R. Teel, and L. Zaccarian. Anti-windup for exponentially unstable linear systems with inputs limited in magnitude and rate. In *Proceedings of the 2000 American Control Conference*, volume 2, pages 1230–1234 vol.2, 2000.

[6] Alec Bateman and Zongli Lin. An analysis and design method for linear systems under nested saturation. *Systems and Control Letters*, 48(1):41–52, 2003.

[7] S. Boyd, L. El Ghaoui, E. Feron, and V. Balakrishnan. *Linear Matrix Inequalities in System and Control Theory*, volume 15 of *Studies in Applied Mathematics*. SIAM, Philadelphia, PA, 1994.

[8] P. Chan, S. F. Catpinar, B. Chang, H. Kwatny, and C. M. Belcastro. Aircraft spiral dive attractors due to actuator saturation. pages 1072–1077. 13th IEEE International Conference on Control Automation (ICCA), July 2017.

[9] Vijay Sekhar Chellaboina, Wassim M. Haddad, and Jin Hyoung Oh. Fixed-order dynamic compensation for linear systems with actuator amplitude and rate saturation constraints. *International Journal of Control*, 73(12):1087–1103, 2000.

[10] Pang-Chia Chen and Jeff S. Shamma. Gain-scheduled $\ell 1$-optimal control for boiler-turbine dynamics with actuator saturation. *Journal of Process Control*, 14(3):263 – 277, 2004.

[11] Mengjia Cui, Zhen Zhang, and Peng Yan. Tracking control of a large range 3d printed compliant nano-manipulator with enhanced anti-windup compensation. *Mechanical Systems and Signal Processing*, 131:33–48, 2019.

[12] Marco Dettori. *LMI techniques for control with application to a Compact Disc player mechanism*. PhD thesis, Delft University of Technology, The Netherlands, 2001.

[13] Michael A. Dornheim. Report pinpoints factors leading to YF-22 crash. (fighter plane prototype). *Aviation Week and Space Technology*, 137(19):53, 1992.

[14] J Doyle, A Packard, and K Zhou. Review of LFTs, LMIs, and μ. In *Proceedings of the 30th IEEE Conference on Decision and Control*, pages 1227–1232, 1991.

[15] Yoshio Ebihara and Tomomichi Hagiwara. New dilated LMI characterizations for continuous-time multiobjective controller synthesis. *Automatica*, 40(11):2003–2009, 2004.

[16] Pascal Gahinet and Pierre Apkarian. A linear matrix inequality approach to H_∞ control. *International Journal of Robust and Nonlinear Control*, 4(4):421–448, 1994.

[17] Sergio Galeani, Sophie Tarbouriech, Matthew Turner, and Luca Zaccarian. A tutorial on modern anti-windup design. *European Journal of Control*, 15(3-4):418–440, 2009.

[18] Ankit Gupta, Hakan Koroglu, and Paolo Falcone. Computation of low-complexity control-invariant sets for systems with uncertain parameter dependence. *Automatica*, 101:330 – 337, 2019.

[19] M.A. Hinostroza, Weilin Luo, and C. Guedes Soares. Robust fin control for ship roll stabilization based on $\mathcal{L}_2$-gain design. *Ocean Engineering*, 94:126 – 131, 2015.

[20] Peter Hippe. *Windup in control: its effects and their prevention.* Springer Science & Business Media, 2006.

[21] Tingshu Hu and Zongli Lin. *Control Systems with Actuator Saturation: Analysis and Design.* Birkhauser Boston, Inc, Secaucus, NJ, USA, 2001.

[22] Tingshu Hu, Zongli Lin, and Ben M Chen. An analysis and design method for linear systems subject to actuator saturation and disturbance. *Automatica*, 38(2):351–359, 2002.

[23] Faryar Jabbari and I Emre Köse. Rate and magnitude-bounded actuators: scheduled output feedback design. *International Journal of Robust and Nonlinear Control*, 14(13-14):1169–1184, 2004.

[24] Vikram Kapila and K Grigoriadis, editors. *Actuator saturation control.* Marcel Dekker, 2002.

[25] I. Emre Köse and Faryar Jabbari. Rate and magnitude-bounded actuators: Scheduled state feedback design. In *15th IFAC World Congress*, pages 73–78. IFAC Proceedings Volumes, 2002.

[26] Ibrahim B. Kucukdemiral. Robust disturbance rejection for discrete-time systems having magnitude and rate bounded inputs. *Journal of the Franklin Institute*, 357(12):8252–8276, 2020.

[27] Ibrahim Beklan Kucukdemiral, Ferdi Cakici, and Hakan Yazici. A model predictive vertical motion control of a passenger ship. *Ocean Engineering*, 186:106100, 2019.

[28] Pengbo Liu, Peng Yan, and Hitay Özbay. Design and trajectory tracking control of a piezoelectric nano-manipulator with actuator saturations. *Mechanical Systems and Signal Processing*, 111:529–544, 2018.

[29] J. Lofberg. YALMIP : A toolbox for modeling and optimization in MATLAB. In *2004 IEEE International Conference on Robotics and Automation*, pages 284–289, 2004.

[30] Ping Lu. Tracking control of nonlinear systems with bounded controls and control rates. *Automatica*, 33(6):1199 – 1202, 1997.

[31] David Q. Mayne. Model predictive control: Recent developments and future promise. *Automatica*, 50(12):2967–2986, 2014.

[32] M. C. De Oliveira, J. C. Geromel, and J. Bernussou. Extended H_2 and H_∞ characterizations and controller parametrizations for discrete-time systems. *International Journal of Control*, 75(9):666–679, 2002.

[33] A. H. K. Palmeira, J. M. Gomes Da Silva, S. Tarbouriech, and I. M. F. Ghiggi. Sampled data control under magnitude and rate saturating actuators. *International Journal of Robust and Nonlinear Control*, 26(15):3232–3252, 2016.

[34] Pablo A. Parrilo. *Structured Semidefinite Programs and Semialgebraic Geometry Methods in Robustness and Optimization*. PhD thesis, California Institute of Technology, 2000.

[35] Goele Pipeleers, Bram Demeulenaere, Jan Swevers, and Lieven Vandenberghe. Extended LMI characterizations for stability and performance of linear systems. *Systems and Control Letters*, 58(7):510 – 518, 2009.

[36] Maryam Sadeghi Reineh, Solmaz S. Kia, and Faryar Jabbari. New anti-windup structure for magnitude and rate limited inputs and peak-bounded disturbances. *Automatica*, 97:301–305, 2018.

[37] C Scherer and S Weiland. *Lecture notes: Linear matrix inequalities in control*. Dutch Institute for Systems and Control, Delft, The Netherlands, 2015.

[38] C. W. Scherer. A full block S-procedure with applications. In *36th IEEE Conference on Decision and Control*, volume 3, pages 2602–2607, Dec 1997.

[39] C.W. Scherer. LMI relaxations in robust control. *European Journal of Control*, 12(1):3 – 29, 2006.

[40] Julio Solís-Daun, Rodolfo Suárez, and José Álvarez Ramírez. Global stabilization of nonlinear systems with inputs subject to magnitude and rate bounds: A parametric optimization approach. *SIAM Journal on Control and Optimization*, 39(3):682–706, 2000.

[41] Lei Song and Jianying Yang. An improved approach to robust stability analysis and controller synthesis for LPV systems. *International Journal of Robust and Nonlinear Control*, 21(13):1574–1586, 2011.

[42] A.A. Stoorvogel and A. Saberi. Editorial (special issue on control problems with constraints). *International Journal of Robust and Nonlinear Control*, 9(10):583–584, 1999.

[43] S Tarbouriech, C Prieur, and J.M.G Da Silva. Stability analysis and stabilization of systems presenting nested saturations. *IEEE Transactions on Automatic Control*, 51(8):1364–1371, 2006.

[44] S. Tarbouriech and M. Turner. Anti-windup design: an overview of some recent advances and open problems. *IET Control Theory and Applications*, 3:1–19, 2009.

[45] S. S. Tohidi, Y. Yildiz, and I. Kolmanovsky. Pilot induced oscillation mitigation for unmanned aircraft systems: An adaptive control allocation approach. In *2018 IEEE Conference on Control Technology and Applications (CCTA)*, pages 343–348, Aug 2018.

[46] Seyed Shahabaldin Tohidi and Yildiray Yildiz. Handling actuator magnitude and rate saturation in uncertain over-actuated systems: a modified projection algorithm approach. *International Journal of Control*, pages 1–14, 2020.

[47] Zhaoyang Wan and Mayuresh V Kothare. An efficient off-line formulation of robust model predictive control using linear matrix inequalities. *Automatica*, 39(5):837–846, 2003.

[48] S. Wang, Y. Gao, J. Liu, and L. Wu. Saturated sliding mode control with limited magnitude and rate. *IET Control Theory Applications*, 12(8):1075–1085, 2018.

[49] Yong Wang and Richard M. Murray. Bifurcation control of rotating stall with actuator magnitude and rate limits: Part I–model reduction and qualitative dynamics. *Automatica*, 38(4):597 – 610, 2002.

[50] Yansheng Yang and Bo Jiang. Variable structure robust fin control for ship roll stabilization with actuator system. In *Proceedings of the 2004 American Control Conference (ACC 2004)*, volume 6, pages 5212–5217, 2004.

[51] Bin Zhou. Analysis and design of discrete-time linear systems with nested actuator saturations. *Systems & Control Letters*, 62(10):871 –879, 2013.

[52] Bin Zhou, Zongli Lin, and Guang-Ren Duan. Global and semi-global stabilization of linear systems with multiple delays and saturations in the input. *SIAM Journal on Control and Optimization*, 48(8):5294–5332, 2010.